



Research article

[urn:lsid:zoobank.org:pub:60245C9C-34EE-4F68-A346-F7A684E18EB6](https://zoobank.org/pub:60245C9C-34EE-4F68-A346-F7A684E18EB6)

**A new highly apomorphic species of *Bujurquina* (Teleostei: Cichlidae)
from a reverse flowing river in the Peruvian Amazon,
with a key to the species in the genus**

Oldřich ŘÍČAN ^{1,*} & Štěpánka ŘÍČANOVÁ²

^{1,2}University of South Bohemia, Faculty of Science, Department of Zoology, Branišovská 31,
370 05, České Budějovice, Czech Republic.

*Corresponding author: oldrich.rican@prf.jcu.cz

²Email: ricanova@prf.jcu.cz

¹[urn:lsid:zoobank.org:author:197D8E32-925D-4A16-8ED1-9E13C74D98D6](https://zoobank.org/author:197D8E32-925D-4A16-8ED1-9E13C74D98D6)

²[urn:lsid:zoobank.org:author:9A90D79A-DBA7-4CF7-86C8-97FEE293F2AC](https://zoobank.org/author:9A90D79A-DBA7-4CF7-86C8-97FEE293F2AC)

Abstract. *Bujurquina* is the most widely distributed and species-rich genus of cichlids in the western Amazon of South America. In this study we describe a new species from Peru from a hypothesized reverse flowing river system. Prior to the origin of the modern Amazon River at 4.5 Ma, this river system had its headwaters on the Iquitos arch, one of several main structural arches (swells) in the Amazon. Prior to the origin of the modern Amazon these arches formed topographic barriers of drainage basins in lowland Amazonia. For our analyses we use morphological and molecular data, analyzed through multivariate statistics and molecular phylogenies, respectively. For all valid species in the genus (except *B. cordemadi* and *B. pardus*) we additionally for the first time provide photographs of live specimens. Based on DNA phylogeny and coloration patterns we demonstrate that *Bujurquina* is divided into two main clades and based on this we provide a dichotomous key for all the species.

Keywords. Biogeography, endemism, freshwater fishes, new species, phylogeny.

Řičan O. & Řičanová Š. 2023. A new highly apomorphic species of *Bujurquina* (Teleostei: Cichlidae) from a reverse flowing river in the Peruvian Amazon, with a key to the species in the genus. *European Journal of Taxonomy* 870: 167–201. <https://doi.org/10.5852/ejt.2023.870.2127>

Introduction

The Amazon basin and especially the western Amazon with the adjacent Tropical Andes are the most biodiverse areas of our planet (Reis *et al.* 2003; Hubbell *et al.* 2008; Hoorn & Wesselingh 2010a, 2010b; Albert & Reis 2011). The Amazon basin hosts by far the most diverse and extreme terrestrial and aquatic ecosystems on Earth. Paramount among its megadiverse groups are the freshwater fishes, by far the largest community of these vertebrates in the World (Reis *et al.* 2003; Albert & Reis 2011; Van der Sleen & Albert 2018). The Amazonian species megadiversity is however still known based on collection of limited area across the vast complex region (Hoorn & Wesselingh 2010a, 2010b), and the sampling is biased towards the navigable rivers and other accessible areas, with the terra firme areas of the lowlands

remaining less explored, especially among the freshwater fishes (Albert & Reis 2011; Crampton 2011; Van der Sleen & Albert 2018; Oberdorff *et al.* 2019).

The lowland Amazon is drained by thousands of kilometers of large and deep (> 5 m mid-channel depth) rivers meandering and anastomosing across broad sunlit floodplains (the floodplain rivers), and by tens of thousands of kilometers of non-floodplain (terra firme) streams and rivers, virtually all flowing mostly under a closed-forest canopy (Toivonen *et al.* 2007; Crampton 2011). The terra firme areas of the western lowland Amazon are ecological islands whose fish faunas are the least known and studied, with virtually all studies of faunal evolution focused on the much better accessible rivers, floodplains, and riparian woodlands (see Albert *et al.* 2018a, 2018b and reference there in). The terra firme islands however have a total area much larger than the much better known areas of the major rivers and their tributaries (the lowland inundable areas) that isolate them (Albert & Reis 2011; Crampton 2011; Van der Sleen & Albert 2018; Oberdorff *et al.* 2019).

Our knowledge of Amazonia's present biodiversity is thus despite being the most diverse part of the planet still very limited, and even more limited is our understanding of its evolution, where the general outlines were derived predominantly from geological and paleontological data while the input from extant faunal data and phylogenies has been very limited (Hoorn & Wesselingh 2010a, 2010b). Of paramount importance for Amazonian evolution appears to have been the Andean orogeny which has shaped the Andes and the river network of western Amazonia and appears to be the main determinant of Amazonian diversity both for the aquatic and terrestrial faunas (Hoorn & Wesselingh 2010a, 2010b; Albert & Reis 2011; Albert *et al.* 2011, 2018a). The originally south-north oriented drainage of the paleo-Amazon changed with progressive Andean elevation and eastward propagation and sedimentation into the present west-east oriented river network. This large-scale reorientation of the Amazon River network must have heavily reshaped the biodiversity patterns and promoted further diversification, both in the foothills as well as in the lowlands. The present mosaic of muddy, clear, and black-water rivers was established from a previous still little known river network preceded in the western Amazon by a mega-wetland, the Pebas formation (Hoorn & Wesselingh 2010a, 2010b; Wesselingh & Hoorn 2011).

The freshwater fishes are the best model group for the study of continental evolution because they are the least dispersal capable larger organisms and hence those most strictly associated with landscape evolution (Wallace 1876; Darlington 1957). There are, however, to this date no well sampled studies that would include phylogenies and focus on groups endemic to the area of the western Amazon.

One of the best groups to study Neotropical biogeography and landscape evolution are the cichlid fishes, which is one of the most important groups of Neotropical fishes. Cichlids are generally highly philopatric, have small-scale endemism and a large species diversity, and are found throughout all the aquatic (or terrestrial) habitats (including the main rivers and their inundation zones but especially the terra firme areas). This combination makes them one of the groups with the largest explanatory power. Cichlids are the dominant group of larger sized fishes in Middle America (Myers 1966; Bussing 1976, 1985; Říčan *et al.* 2013, 2016) and the third richest family of fishes in South America (Van der Sleen & Albert 2018).

Among the cichlid fishes the best model group to study specifically the Andean and western Amazonian biogeography and landscape evolution and its direct influence on the formation of biodiversity is the genus *Bujurquina* Kullander, 1986. This is because *Bujurquina* is the only cichlid genus whose geographical distribution and diversity is almost limited to the western Amazon and its distribution and endemism follows the putative course of the paleo-Amazon (Kullander 1986; Říčan 2017; Říčan *et al.* 2022). *Bujurquina* thus has a distribution unlike any other of the species rich genera of South American cichlids (except *Apistogramma* Regan, 1913), which generally have highest diversity and endemism in

the older eastern Amazon in the Brazilian and Guiana shield areas (Stawikowski & Werner 1998, 2004; Kullander *et al.* 2018; Van der Sleen & Albert 2018; Říčan *et al.* 2021).

The distribution of *Bujurquina* follows an arc from the south in Argentina, Paraguay, Brazil and Bolivia, through its highest currently known centers of diversity and endemism in Peru and Ecuador, and continues to the north into Colombia and Venezuela (Kullander 1986; Říčan *et al.* 2022). *Bujurquina* exemplifies a typical cichlid group with highly pronounced philopatry, small-scale endemism, and strong adaptation to local environmental conditions (Říčan 2017; Říčan *et al.* 2022). Molecular-based dating of *Bujurquina* diversification (Musilová *et al.* 2015; Říčan *et al.* 2022) supports the hypothesis that most of its evolution occurred right through the time period of major Amazonian river network reorganization described above.

Bujurquina is thus, due to its time frame of evolution, geographical distribution, species diversity and narrow endemism, one of the best candidate groups among the cichlid fishes and likely among all fish groups to study both group-specific and general patterns and processes in the evolution of western Amazonia (Říčan *et al.* 2022). Understanding diversity patterns and evolution of *Bujurquina* will thus not only strengthen our understanding of the processes of cichlid and fish diversification in this area but may also provide a groundwork for analysing faunal and biogeographical evolution of the whole western Amazon.

The biogeography and endemism of *Bujurquina* plays out in two biogeographic zones. There is a separate band of endemism in *Bujurquina* in the Andean foothills, which has a distinct fauna from the supposedly more widely distributed species in the Amazonian lowlands (Kullander 1986; Říčan *et al.* 2022). The two zones host different faunas of *Bujurquina* since the lowland species are usually not known from the adjacent foothills and vice versa (Kullander 1986). Foothill areas of the same river basins thus as a rule have a different *Bujurquina* fauna from lowland areas of the same basins (Kullander 1986; Říčan 2017; Říčan *et al.* 2022).

Bujurquina currently includes 18 described species, but this species diversity is clearly significantly underestimated as is outlined and demonstrated in this study and in parallel studies (Říčan *et al.* 2022). If we generalize the biogeographic pattern to all described species of *Bujurquina* (i.e., not only those found in Peru) the foothill endemic species are: *B. eurhinus* Kullander, 1986 (Madeira basin, Peru), *B. robusta* Kullander, 1986, *B. labiosa* Kullander, 1986, *B. megalospilus* Kullander, 1986, *B. apoparuana* Kullander, 1986, *B. hophrys* Kullander, 1986 (all Ucayali basin, Peru), *B. huallagae* Kullander, 1986, *B. ortegai* Kullander, 1986, *B. zamorensis* (Regan, 1905), *B. pardus* Arbour, Barriga Salazar & López-Fernández, 2014 (all Marañón basin, Peru and Ecuador), and the northernmost species *B. mariae* (Eigenmann, 1923) (Orinoco basin in Colombia and Venezuela). The lowland band of species, which also includes the supposedly more widely distributed species includes *B. vittata* (Heckel, 1840) (Paraguay basin, Argentina, Paraguay and Bolivia), *B. oenolaemus* Kullander, 1987 (Paraguay basin, Bolivia), *B. cordemadi* Kullander, 1986, *B. tambopatae* Kullander, 1986 (all Madeira basin, Peru and possibly Bolivia), *B. moriorum* Kullander, 1986 (type in lower Ucayali basin, Peru), *B. peregrinabunda* Kullander, 1986, and *B. sypilus* (Cope, 1872) (both with types in the Amazon proper in Peru).

In this study we describe a new highly apomorphic species of *Bujurquina* from the lowland Amazon of Peru (Loreto) and we demonstrate its distinctiveness using morphological and molecular data, analyzed through molecular phylogenies and multivariate statistics, respectively. This species description is the first contribution in a series that aims to describe many new species in the genus that have been discovered in studies parallel to this one, with the majority of the new species with type localities in Ecuador, several of them shared with Peru, and also species apparently endemic to Peru and Colombia.

Material and methods

Species determination

We combine morphological species determination with post-hoc species delimitation using the molecular mtDNA cytochrome b (*cytb*) marker. Specimens were identified to species with the use of original descriptions, identification keys, and comparative material of all presently recognized species of *Bujurquina*.

The Unified Species Concept was employed in the present study (de Queiroz 2007) in which species are equated with independently evolving metapopulation lineages. Our operational species-delimitation criteria were consistent morphological differences together with topology and divergence analyses in molecular phylogeny.

Specimen sampling

We have collected a representative sampling of specimens and tissue samples covering the whole distribution of *Bujurquina* with particular focus on the Peruvian Amazon, especially in the more diverse and accessible foothills. Our molecular sampling in this study includes 13 of the 18 valid species, with most described species sampled from or close to their type localities (Figs 1–5; [Supp. file 1](#): Table S1; [Supp. file 2](#): Fig. S1), while our morphological analyses include all valid species. In addition to the described species our sampling includes several putative undescribed species, one of which is described in this study.

The fish specimens and tissue samples were collected by the first author under permanent permits to Hernán Ortega (Universidad Nacional Mayor de San Marcos, Lima, Perú), Cecilia Elizabeth Rodriguez Haro (IKIAM, Tena, and UEA, Puyo, Ecuador), and Javier Maldonado Ocampo (Universidad Javeriana, Bogota, Colombia). Specimens were obtained by fishing using gill nets, cast nets and hook and line in all recognizable microhabitats at all localities (following the recommendations of Říčan 2017). Localities were chosen specifically so that they capture the full regional ecological habitat variation of the studied area. At localities with sufficient visibility (all visited upland and rainforest streams and some lowland locations) direct observation of the fish fauna was carried out using mask and snorkel.

Collected specimens ([Supp. file 1](#): Table S1) were individually and permanently tagged and a DNA tissue sample taken from their right pelvic fin. DNA tissue samples were preserved in 1.5 ml Eppendorf Safe lock tubes in absolute ethanol and for the duration of our studies on this genus deposited together with the specimens at the fish collection of the Department of Zoology, Faculty of Science, University of South Bohemia in České Budějovice, Czech Republic. Specimens were preserved in 10% formalin and later transferred to 70% ethanol. Type specimens of the newly described species are deposited at MUSM (Museo de Historia Natural, Universidad Nacional Mayor de San Marcos), Lima, Peru.

Morphological methods

Counts were taken as in Kullander (1986). Measurements were taken as described by Kullander (1986) and the pattern of their variation was visualized using principal component analysis (PCA) implemented in Canoco 5 (Microcomputer Power, Ithaca, NY, USA) according to Šmilauer & Lepš (2014). Measurements were taken as straight line distances with digital calliper to 0.1 mm on left side of specimen. Body length is expressed as standard length (SL). Morphometric characters are expressed as percents of the SL. For PCA analyses of proportional morphometric measurements only fully grown specimens above 60 mm SL and with a similar size range were used. Lower pharyngeal jaw (LPJ) shape was studied using four linear measurements following Hellig *et al.* (2010): LPW (Lower Pharyngeal Width) – distance between the tips of the lateral processes; LPL (Lower Pharyngeal Length) – measured from the rostral tip of the pharyngeal element in a perpendicular relative to the line connecting the

lateral processes; PDW (dentigerous width) – distance between the lateral margins of the right and left most lateral teeth along the posterior edge of the dentigerous area; PDL (dentigerous length) – distance between the rostral margin of the most rostral teeth and the caudal margin of the most caudal teeth. For PCA analysis these measurements were combined into three proportional measurements: L/W ratio (LPL/LPW), Ld/Wd ratio (PDL/ PDW), and Ld/W ratio (PDL/ LPW). Additionally, the thickness of the LPJ excluding the teeth was measured at the posterior end at the suture of the LPJ. Scale row nomenclature follows Kullander (1996). E1 scale counts refer to the scales in the row immediately above that containing the lower lateral line (Lucena & Kullander 1992). Body bar terminology follows Řičan *et al.* (2005). In the descriptions, the number of specimens is indicated in parentheses, the holotype is indicated by an asterisk. Institutional abbreviations are as listed in Ferraris (2007) and Sabaj (2020).

List of studied species and specimens is in [Supp. file 1](#): Table S1 and tables of morphometric data are in [Supp. file 2](#): Table S2.

Molecular marker

For molecular phylogenetic analyses and delimitation of putative species we have used the mitochondrial (mtDNA) cytochrome *b* (*cytb*) gene. The *cytb* is the single most often used molecular marker in cichlid

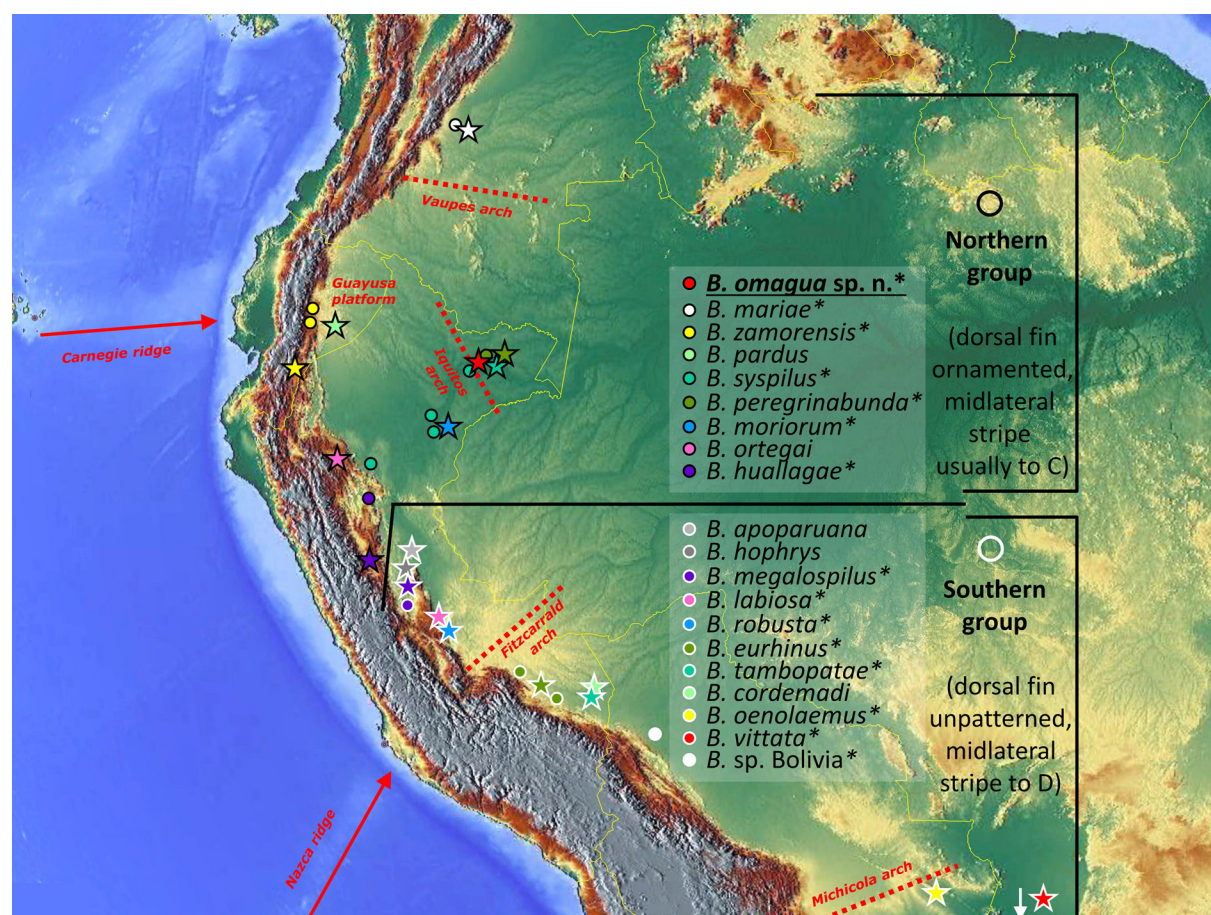


Fig. 1. Distribution and the two main groups of species of *Bujurquina* Kullander, 1986. Shown with red dotted lines are main geographic drainage basin divides (structural arches) of the western Amazon. Red arrows show the two main subducting ridges responsible for the origin of the formation of the structural arches of the western Amazon. All species were included in morphological analyses, species with an asterisk were also available for molecular analyses. Stars denote type localities for valid species.



Fig. 2. Representative live specimens of the valid species of *Bujurquina* Kullander, 1986 (plus *B. sp. Bolivia*) in the Southern group (no photo of a live specimen of *B. cordemadi* Kullander, 1986 is available and we are not aware that the species has ever been reliably identified and photographed alive).

phylogenetic studies and has been one of the first molecular markers to provide well resolved phylogenies of the Neotropical cichlids that have subsequently been virtually completely confirmed by later studies including recent phylogenomic studies (e.g., Říčan *et al.* 2016; Ilves *et al.* 2017; Burress *et al.* 2018a, 2018b). The *cytb* has recently been used with great success in similar studies focusing on diversity of cichlids in South America in two other genera (Piálek *et al.* 2019a, 2019b; Říčan *et al.* 2019, 2021).

For the molecular *cytb* marker we have sequenced 82 specimens from the 22 ingroup species and species-level taxa, and we also include several sequences from our previous studies (Musilová *et al.* 2008, 2009) and a few available from other studies as deposited in GenBank (Supp. file 1: Table S1). The total number of ingroup sequences is 93 plus outgroup sequences including one heroine genus (*Hypselecara* Kullander, 1986) as the primary outgroup and five cichlasomatine genera (same tribe as *Bujurquina*), including the two successive sister genera of *Bujurquina*, i.e., *Tahuantinsuyoia* Kullander, 1986 and *Andinoacara* Musilová, Říčan & Novák, 2009 (Supp. file 1: Table S1).



Fig. 3. Detailed photographs of the spinous portion of the dorsal fin of species of *Bujurquina* Kullander, 1986 in the Southern group (see Figs 1–2). Note lack of patterning as opposed to various types of ornamentation in species of the Northern group. Note differences in the coloration of the dorsal fin lappets between some of the species, e.g., red-orange, vs white vs black.

Laboratory methods

Genomic DNA was extracted from ethanol-preserved gill or fin tissue using the JETQUICK Tissue DNA Spin Kit (Genomed, Germany) following standard protocol. The primers and reaction conditions of polymerase chain reaction (PCR) amplification are as in Řičan *et al.* (2008). The products were analyzed in an ABI 3730XL automated sequencer (Applied Biosystems, Macrogen Inc., Korea). Contiguous sequences of the gene segments were created by assembling DNA strands (forward and reverse) using GENEIOUS ver. 11.0.2 (<http://geneious.com>, Kearse *et al.* 2012). Nucleotide coding sequences were also translated into protein sequences to check for possible stop codons or other ambiguities. All newly generated sequences were submitted to GenBank under Accession numbers OP436070–OP436254 (Supp. file 1: Table S1). Sequences were aligned using MUSCLE ver. 3.8 (Edgar 2004), using the default settings.



Fig. 4. Representative live specimens of the valid species of *Bujurquina* Kullander, 1986 in the Northern group including the newly described species *B. omagua* sp. nov.

Phylogenetic methods

Maximum parsimony (MP) and neighbor joining (NJ) analyses in PAUP* ver. 4b.10 (Swofford 2003) and Bayesian inference analyses (BI) in MrBayes ver. 3.1.2 (Huelsenbeck & Ronquist 2001; Ronquist & Huelsenbeck 2003) and BEAST ver. 1.8.4 (Drummond & Rambaut 2007) were used for phylogenetic inference. The MP phylogenetic analyses in PAUP* were run with 500 random sequence additions, 10 trees kept per addition, and a hs (heuristic) search on the saved trees to find all the shortest trees. Bootstrap analyses were done using the same approach, with five random sequence additions per one replication. Bootstrap analyses were run with 1000 replications. The BI analyses in MrBayes (and BEAST, see below) were run with haplotype dataset and were partitioning into codon positions (1st+2nd vs 3rd). The haplotype dataset was created in Fabox (Villesen 2007). An optimal model of evolution according to Akaike criterion was selected using MrModeltest ver. 2.2 (Nylander 2004) and PAUP* ver. 4.0b10 (Swofford 2003). The BI analysis using the Markov chain Monte Carlo (MCMC) simulation was run for 2 million generations with trees sampled and saved every 1000 generations. Two independent analyses, each comprising two runs with eight chains, were performed to compare results of independent analyses. The analyses were run at the freely available Cipres server (<https://www.phylo.org/>). The first 10% of trees from each run were discarded as burn-in. Convergence of the runs was estimated with



Fig. 5. Detailed photographs of the spinous portion of the dorsal fin of species of *Bujurquina* Kullander, 1986 in the Northern group (see Figs 1 and 4). Note two main types of patterning of the dorsal fin, a blotched patterning vs lines in the spinous portion of the dorsal fin. Note additional differences in patterning of the spinous portion of the dorsal fin between the species, such as different numbers of lines per membrane, their thickness or angle. Also note differences in the coloration of the dorsal fin lappets between some of the species.

the use of graphical visualization and diagnostics (especially the effective sample size; ESS) in Tracer ver. 1.8.4 (Rambaut & Drummond 2007). The remaining trees were used for reconstruction of the 50% majority-rule consensus tree with posterior probability (PP) values of the branches. Trees were rooted with a representative sampling of heroine and cichlasomatine cichlids including the most closely related genera *Tahuantinsuyoa* and *Andinoacara*.

Molecular clock dating analyses in BEAST

For divergence time estimation we used the Bayesian Evolutionary Analysis by Sampling Trees (BEAST) software package version ver. 1.8.4 (Drummond & Rambaut 2007) with parameters as in MrBayes analyses (except for 30 million generations). We used the relaxed molecular clock model with lognormal distribution of rates and for tree prior the coalescent model with constant size. The calibration of the molecular clock was performed using secondary calibration from the study of Musilová *et al.* (2015) which focused on the dating of Neotropical cichlids in general and the Cichlasomatine cichlids in particular, with focus on *Andinoacara*, the sister-group of the *Bujurquina*–*Tahuantinsuyoa* clade. Musilová *et al.* (2015) employed a calibration using a set of Neotropical fossil cichlid species and is so far the only study that includes *Bujurquina* and its most closely related genera in a dated phylogeny. For the calibration we have used three nodes from the study (Supp. file 2: Fig. S2), 1) the *Andinoacara* basal node, estimated by Musilová *et al.* (2015) at 19.33 Ma (95% HPD 15.03–24.25 Ma), 2) the *Bujurquina*–*Tahuantinsuyoa*–*Andinoacara* node, estimated at 31.51 Ma (95% HPD 26.22–37.17 Ma), and 3) the *Bujurquina*–*Tahuantinsuyoa*–*Andinoacara* vs rest of cichlasomatine cichlids node, estimated at 46.47 Ma (95% HPD 40.96–52.62 Ma).

These analyses were also run at the freely available Cipres server (<https://www.phylo.org/>). Runs were checked for convergence with Tracer ver. 1.8.4 (Rambaut & Drummond 2007). Four well converged runs were combined in LogCombiner ver. 1.8.4 with a burn-in of 10% for each of the data partition schemes. The final tree for each data partition scheme was produced from these data with TreeAnnotator ver. 1.8.4.

Results

Taxonomy

Class Actinopterygii Klein, 1885
Order Cichliformes R. Betancur-R *et al.* 2013
Family Cichlidae Bonaparte, 1835
Genus *Bujurquina* Kullander, 1986

Bujurquina omagua sp. nov.

[urn:lsid:zoobank.org:act:8E478708-58F1-4E97-960C-9FCD93107C9A](https://zoobank.org/urn:lsid:zoobank.org:act:8E478708-58F1-4E97-960C-9FCD93107C9A)

Figs 6–10; Table 1

Bujurquina sp. Oran Řičan *et al.* 2022.

Bujurquina sp. Peru 1 Řičan *et al.* 2022.

Diagnosis

Bujurquina omagua sp. nov. is highly apomorphic compared to other described species in the genus because it is unique in several character states. These include: 1) shape and pattern of the suborbital stripe in adults, which is bend and with a blotch at the postero-ventral end (vs straight or absent, with or without a blotch), with an ontogenetic change with juveniles and subadults having a straight stripe running diagonally postero-ventrally and starting from below the eye in juveniles (i.e., not bend as in adults) and without a blotch, 2) orange cheek and lower head coloration with alternating opalescent lines and series of spots on snout and spotted on cheek and lower head, 3) spinous portion of dorsal fin with a

single thin diagonal black line per membrane, or two lines per membrane in holotype and largest adults (vs unpatterned in all Southern group species, or with circular blotches, with several thick diagonal black lines per membrane, or two thick horizontal bands across the dorsal fin in all other Northern group species), 4) longest snout of all species without overlap (mean 15.5%, 14.4–16.4% of SL; followed by *B. oenolaemus* with a mean of 11.4%, 10.3–13.1 of SL), and 5) most delicate LPJ, expressed by being shortest of all species with widest horns (length/width ratio 0.42–0.45 vs 0.50–0.64 in all other species), one of the smallest dentigerous areas (length of dentigerous area/width of LPJ ratio 0.33–0.34 vs 0.34–0.44 except *B. tambopatae*, *B. moriorum* and *B. huallagae* where also 0.33–0.34), and the least robust dorso-ventrally (bone at posterior end of dentigerous area less thick or equal to length of largest posterior teeth vs much thicker than teeth in other species).

Bujurquina omagua sp. nov. is additionally diagnosed by the following unique combination of morphometric characters, the most pronounced of which characterize the robust head of the species: 1) second to third longest head (after *B. oenolaemus* and together with *B. labiosa*; both with a mean 37.0%, 36.3–38.0% of SL in *B. omagua* vs mean 39.1%, 38.6–40.4% of SL), 2) third longest preorbital distance (after *B. robusta* and *B. oenolaemus*; mean 9.3%, 8.5–10.0% of SL), 3) large interocular distance (largest mean value of all species, 12.5% of SL vs 9.7–12.4% however with large overlap of ranges with the other species), 4) rather wide head (mean 19.9%, range 19.1–20.7% of SL), 5) rather long preorbital distance (mean 9.3%, range 8.5–10.0% of SL, third longest based on mean value), 6) robust head which has rather small eyes (mean 11.3%, range 10.3–12.0% of SL), 7) very deep body (mean 45.1%, range 43.2–46.8% of SL, based on mean the second after *B. vitatta*), but 8) with rather long and shallow caudal peduncle (CPL mean 13.8%, range 12.6–15.6% of SL; CPD mean 16.6%, range 15.5–17.1% of SL), and 9) rather short last spine in the dorsal fin (mean 15.6%, range 12.3–17.1% of SL).

Etymology

The specific epithet ‘*omagua*’ is a noun in apposition given after the Omagua people, which were at the time of first contact with Europeans in the 16th century the dominant people along the banks of the Amazon River upstream from the mouth of the Negro River well into Peru.

Type material

Holotype

PERU • adult ♂, 97.4 mm; Amazonas river basin, Department Loreto, Maynas Province, District Las Amazonas, close to Oran village, Quebrada Sabalillo, cabeceras upper locality P18-17; 3°27′08.4″ S, 72°29′11.8″ W; 97 m a.s.l. based on GPS, 115 m a.s.l. based on Google Earth; 28 Jun. 2018; Řičan leg.; clear-water stream with blackish tinge; ID tag 1189; MUSM 70225 (Figs 6, 8–9).

Paratypes

All from Peru, Amazonas river basin, Department Loreto, Maynas Province, District Las Amazonas, close to Oran village, 9 ex.

PERU • 1 adult, 78.6 mm; same collection data as for holotype; ID tag 1188; GenBank: OP436199; MUSM 70224 • 1 adult, 98.9 mm; same collection data as for holotype; ID tag 1190; GenBank: OP436200; MUSM 70226 (Figs 7–9) • 1 adult, 69.7 mm; same collection data as for holotype; ID tag 1191; GenBank: OP436201; MUSM 70227 (Fig. 7) • 1 adult, 77.1 mm; same collection data as for holotype; ID tag 1192; GenBank: OP436202; MUSM 70228 (Fig. 7) • 1 adult, 78.7 mm; Amazonas river basin, Department Loreto, Maynas Province, District Las Amazonas, close to Oran village, Quebrada Sabalillo on trail from mouth, P18-15; 3°27′45.6″ S, 72°29′22.5″ W; 90 m a.s.l. based on GPS, 110 m a.s.l. based on Google Earth; 27 Jun. 2018; Řičan leg.; clear-water stream with blackish tinge; ID tag 1182; GenBank: OP436196; MUSM 70221 (Figs 7, 9) • 1 adult, 79.9 mm; Amazonas river basin, Department Loreto, Maynas Province, District Las Amazonas, close to Oran village, cabeceras

of Quebrada Sabalillo, lower loc., P18-16; 3°27'17.5" S, 72°29'22.8" W; 75 m a.s.l. based on GPS, 117 m a.s.l. based on Google Earth; 28 Jun. 2018; Řičan leg.; clear-water stream with blackish tinge; ID tag 1185; GenBank: OP436197; MUSM 70222 (Figs 7, 10) • 1 adult, 92.6 mm; same collection data as for preceding; ID tag 1186; GenBank: OP436198; MUSM 70223 (Fig. 7) • 1 adult; Amazonas river basin, Department Loreto, Maynas Province, District Las Amazonas, close to Oran village, small unnamed quebrada just before entering Oran creek, P18-21; 3°27'21.2" S, 72°30'43.2" W; 82 m a.s.l. based on GPS, 104 m a.s.l. based on Google Earth; 3 Jul. 2018; Řičan leg.; clear-water stream with blackish tinge; ID tag 1200; GenBank: OP436204; MUSM 70229 (Fig. 7) • 1 juvenile; same collection data as for preceding; GenBank: OP436205; MUSM 70230.

Description

Compound, based on eight specimens from Sabalillo creek, 69.7–98.9 mm. Refer to Figs 6–10. Measurements summarized in Table 1.

SHAPE. Moderately elongate, rather robust, deep bodied (body depth mean 45.1%, range 43.2–46.8% of SL). Head especially robust, long (head length mean 37.0%, 36.3–38.0% of SL), wide (head width mean 19.9%, range 19.1–20.7% of SL), with large interocular distance (mean 12.5%, range 11.6–14.2% of SL). Frontal outline straight, nape and snout curved, anterior half of dorsal-fin base contour curved. Ventral outline curved. Snout long (mean 15.5%, 14.4–16.4% of SL). Preorbital distance long (mean 9.3%, range 8.5–10.0% of SL), preorbital bone much longer than high. Robust head with rather small eyes (mean 11.3%, range 10.3–12.0% of SL). Lips rather narrow, not turgid. Corner of mouth not reaching vertical from anterior margin of orbit, especially in largest specimens. Rather long and shallow caudal peduncle (CPL mean 13.8%, range 12.6–15.6% of SL; CPD mean 16.6%, range 15.5–17.1% of SL), and rather short last spine in dorsal fin (mean 15.6%, range 12.3–17.1% of SL).

SCALES. Squ. long. (E1) scales 24 (5), 25 (3); 2 scales between L1 and dorsal fin anteriorly, 2 scales between L1 and L2. Upper lateral line (L1) with 15 (1), 16 (7) scales. Lower lateral line (L2) with 9 (4), 10 (3), 11 (1) scales; canal bearing scales on caudal fin: 0 in dorsal, 0-1 in median and 0 in ventral sequence. Cheek scales in 3 (8) series. Anterior portion of caudal fin scaly.

FINS. Dorsal fin XII.11 (1), XIII.10 (1), XIII.11 (1), XIV.9 (1), XIV.10 (4). Soft anal fin pointed, 3rd ray longest, reaching to middle of caudal fin or slightly beyond. Anal fin III.8 (8). Pectoral fin with rounded tip, reaching to above genital papilla to anal-fin origin (to 2nd spine in one specimen); Pectoral fin 13 (8). Pelvic fin pointed, first ray slightly produced, reaching to origin of anal fin or base of 1st spine of anal fin. Caudal fin rounded, without well-developed streamers or with only short streamers.

GILL-RAKERS. 1 epibranchial, 1 in angle, and 5 (3), 6 (4), 7 (1) ceratobranchial rakers externally on first arch.

JAW TEETH. An outer series of stronger, conical, sharply pointed, slightly recurved teeth, slightly increasing in size anteriorly, not worn, 15–22 in outer hemiseries in upper jaw.

LOWER PHARYNGEAL JAW AND TEETH. Lower pharyngeal jaw (LPJ) as examined in two specimens (79.8–98.9 mm) (Fig. 10) very delicate, most delicate LPJ of all described species of *Bujurquina*, very shallow vertically dorso-ventrally (bone at posterior end of dentigerous area less thick than length of largest posterior teeth in the smaller specimen, almost so in the larger specimen vs thicker than the teeth in all other species). LPJ also shortest and widest of all species, length/width ratio 0.42–0.45 (vs 0.50–0.64 in all other species). LPJ tooth-plate (due to the longest arms within *Bujurquina*) also one of the shortest in genus, length of dentigerous area/width of LPJ ratio 0.33–0.34 (vs 0.34–0.44 except *B. tambopatae*, *B. moriorum* and *B. huallagae* where also 0.33–0.34), Teeth slightly laterally compressed (most

pronounced in posterior row), slightly bicuspid with main cusp posterior, central and posterior teeth largest, smaller towards outside, central teeth with flat-worn apex, others with pronounced tip.

Coloration in alcohol

Coloration limited to melanin patterns in preserved state, ground colour light yellowish-brownish, lighter towards whitish on chest and anterior abdomen, dusky greyish on anterior head, snout, and dorsum. Dark diffuse and wide interorbital band. Operculum silvery greyish.

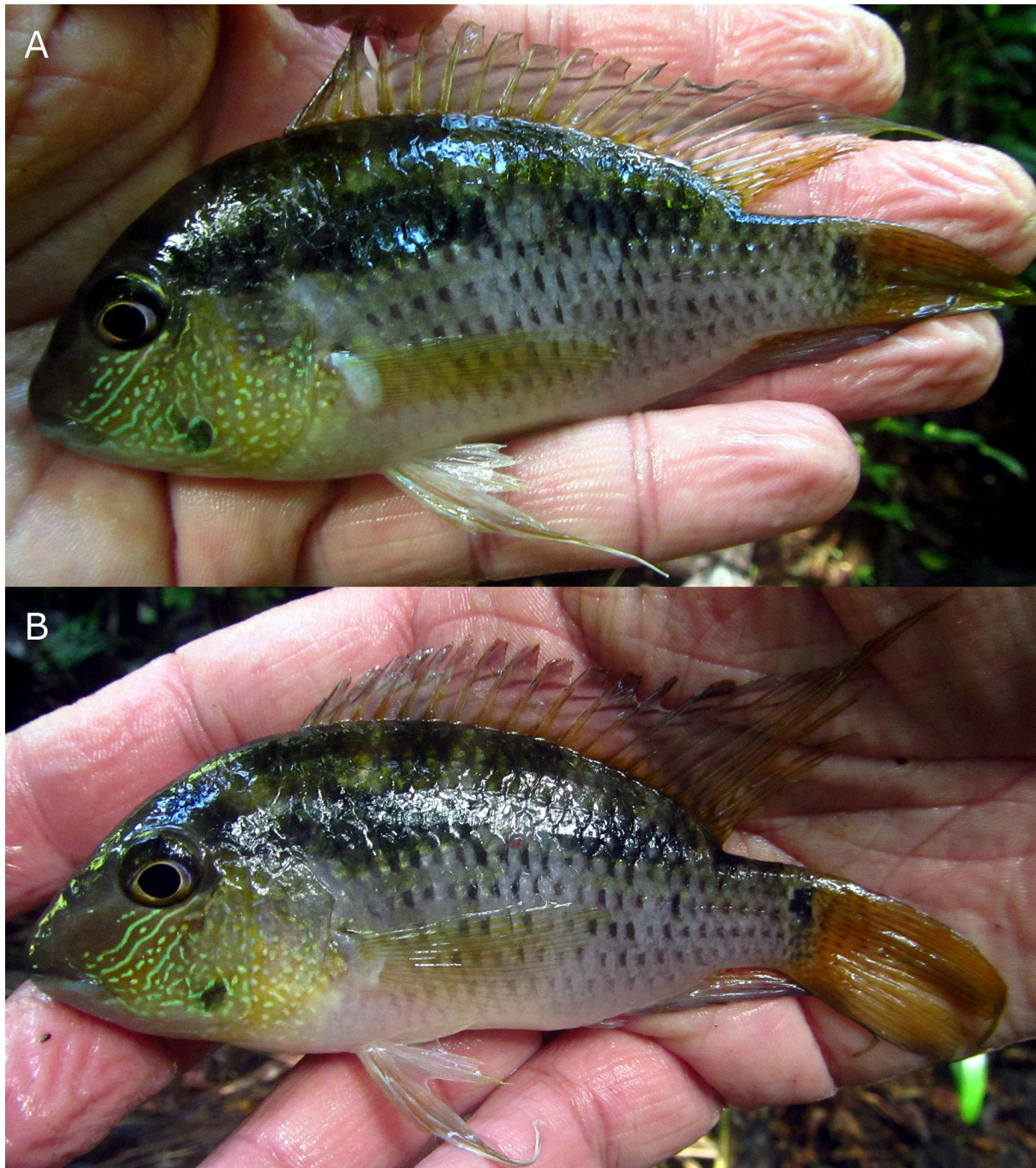


Fig. 6. *Bujurquina omagua* sp. nov., holotype (MUSM 70225), 97.4 mm, ID tag 1189, Quebrada Sabalillo, cabeceras upper loc. P18-17 (3°27'08.4" S, 72°29'11.8" W). **A.** Left side. **B.** Right side reversed.

Table 1. Proportional measurements in percent of standard length of nine specimens of *Bujurquina omagua* sp. nov. larger than 60 mm SL. Abbreviation: SD = standard deviation.

	<i>B. omagua</i> sp. nov.					
	Holotype	Mean	Range		SD	n
			min	max		
Standard length (mm)	97.4	84.1	69.7	98.9		8
Head length	36.3	37.0	36.3	38.0	0.69	8
Snout length	16.3	15.5	14.5	16.4	0.84	8
Body depth	43.2	45.1	43.2	46.8	1.00	8
Orbital diameter	10.3	11.3	10.3	12.0	0.66	8
Head width	19.7	19.9	19.1	20.7	0.64	8
Interorbital width	12.6	12.5	11.6	14.2	0.90	8
Preorbital depth	9.6	9.3	8.5	10.0	0.54	8
Caudal-peduncle depth	15.5	16.6	15.5	17.1	0.52	8
Caudal-peduncle length	12.7	13.8	12.6	15.6	1.05	8
Pectoral-fin length	33.3	33.4	32.4	34.8	0.81	8
Pelvic-fin length	36.0	35.9	30.1	39.5	2.92	8
Last dorsal-fin spine length	15.7	15.6	12.3	17.1	1.59	8

Up to four clearly defined grey lines between eye and mouth corner and on anterior cheek interspersed with spots, rest of cheek as well as opercular series richly spotted. Suborbital stripe rather narrow and of uniform width, diffuse and ghost-like, bend from behind eye forward to cheek and then postero-ventrally to a variously developed suborbital stripe blotch in adults (never ocellated and with diffuse borders). In one collected juvenile specimen and in subadults straight (i.e., not bend), running from below eye (vs from behind eye) diagonally postero-ventrally.

Midlateral band continuous from head to penultimate vertical bar on body, strongly pigmented and black, very wide anteriorly and gradually narrowing posteriorly. No interruption in vertical bar 5 (sensu Řičan *et al.* 2005), midlateral blotch (usually present and dominant in bar 5 in cichlasomatine cichlids) is absent. Lateral band continued on head across nape close behind eye.

Body with five vertical bars plus one caudal peduncle bar and a caudal peduncle blotch (usually vertically elongated). The five body bars correspond to ontogenetic bars 2–5 with the anteriormost ontogenetic bars 6–7 fused into one wide bar below midlateral band but visible as two above it. Posterior body bars (2–4) narrow and tightly spaced, anterior bars (5, 6+7) wide and widely spaced. Bars darkest dorsally, reaching ventrally approximately to level of lower edge of caudal peduncle. Bars do not extend onto dorsal fin.

Body scale centres (below midlateral band) with dark blotches, more pronounced in zones of vertical bars.

Dorsal fin light grey, lappets indistinct, with a single narrow grey diagonal stripe per membrane in spinous part, with blotches on ventral portion of soft part. Anal fin light grey, with spots on last about four membranes. Caudal fin light grey with minute slightly elongate dark dots on anterior half, distally membranes hyaline with grey edges. Pelvic fin light grey, edge and produced portion of first ray white.

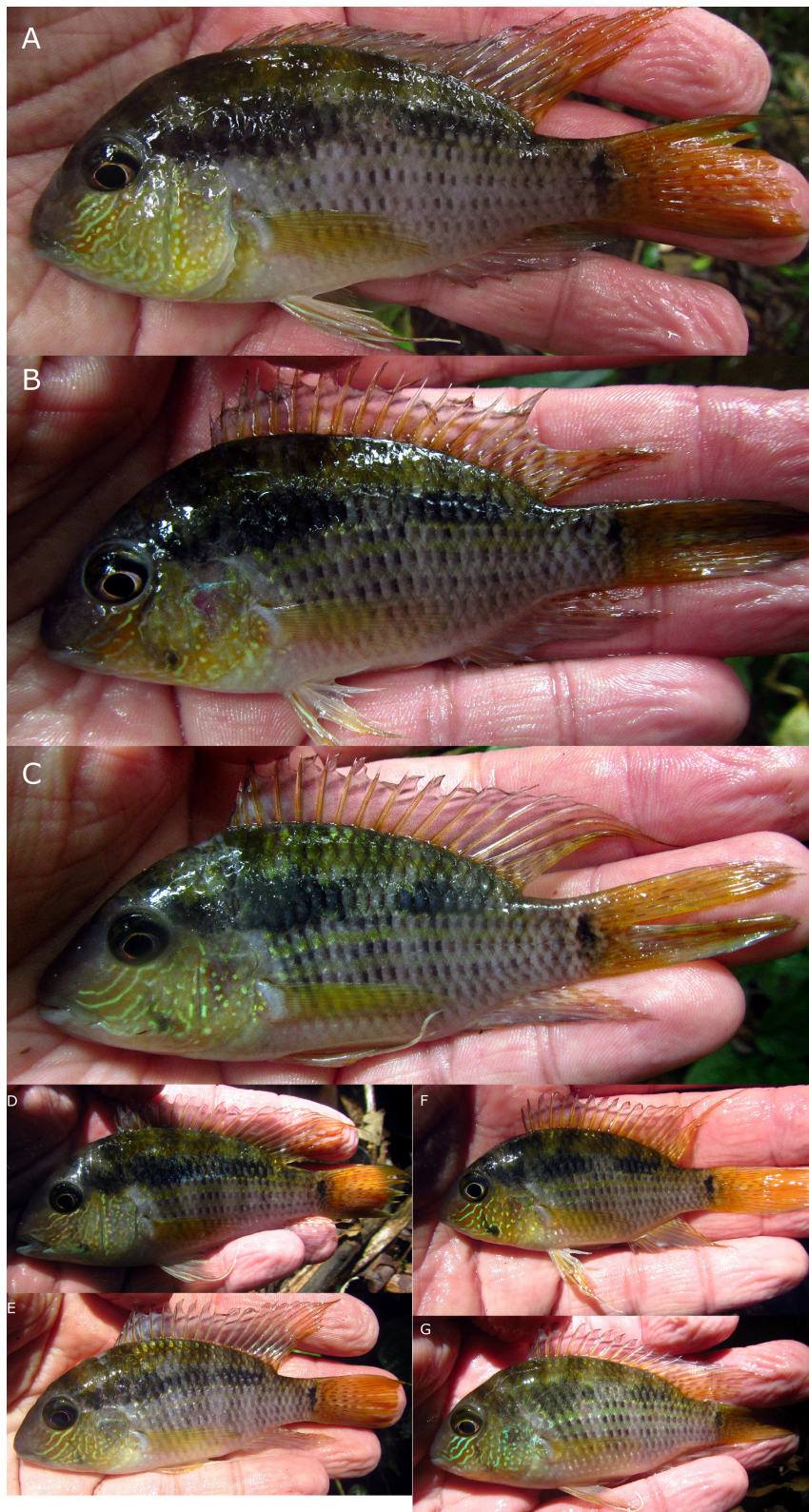


Fig. 7. *Bujurquina omagua* sp. nov., paratypes. **A.** MUSM 70223, P18-16_1186, 92.6 mm. **B.** MUSM 70222, P18-16_1185, 79.9 mm. **C.** MUSM 70221, P18-15_1182, 78.7 mm. **D.** MUSM 70226, P18-17_1190, 98.9 mm. **E.** MUSM 70229, P18-21_1200. **F.** MUSM 70227, P18-17_1191, 69.7 mm. **G.** MUSM 70228, P18-17_1192, 77.1 mm.

Coloration in life

Melanin patterns as in preserved. Lower head, cheek, and opercular series yellow-orange, with opalescent golden to azure blue lines and spots, arranged as up to four clearly defined lines between eye and mouth corner and on anterior cheek interspersed with spots, rest of cheek as well as opercular series richly spotted. Fins orange, pelvic fin yellow, edge and produced portion of first ray white (opalescent). Spinous portion of dorsal fin with a single thin diagonal black line per membrane in juveniles and subadults, and with two lines per membrane in holotype and large adults. Lower lip pale greyish to indistinctly light azure blue. Midlateral blotch present only as a paler reflective area within the dark midlateral band (hence absent from coloration of preserved specimens).

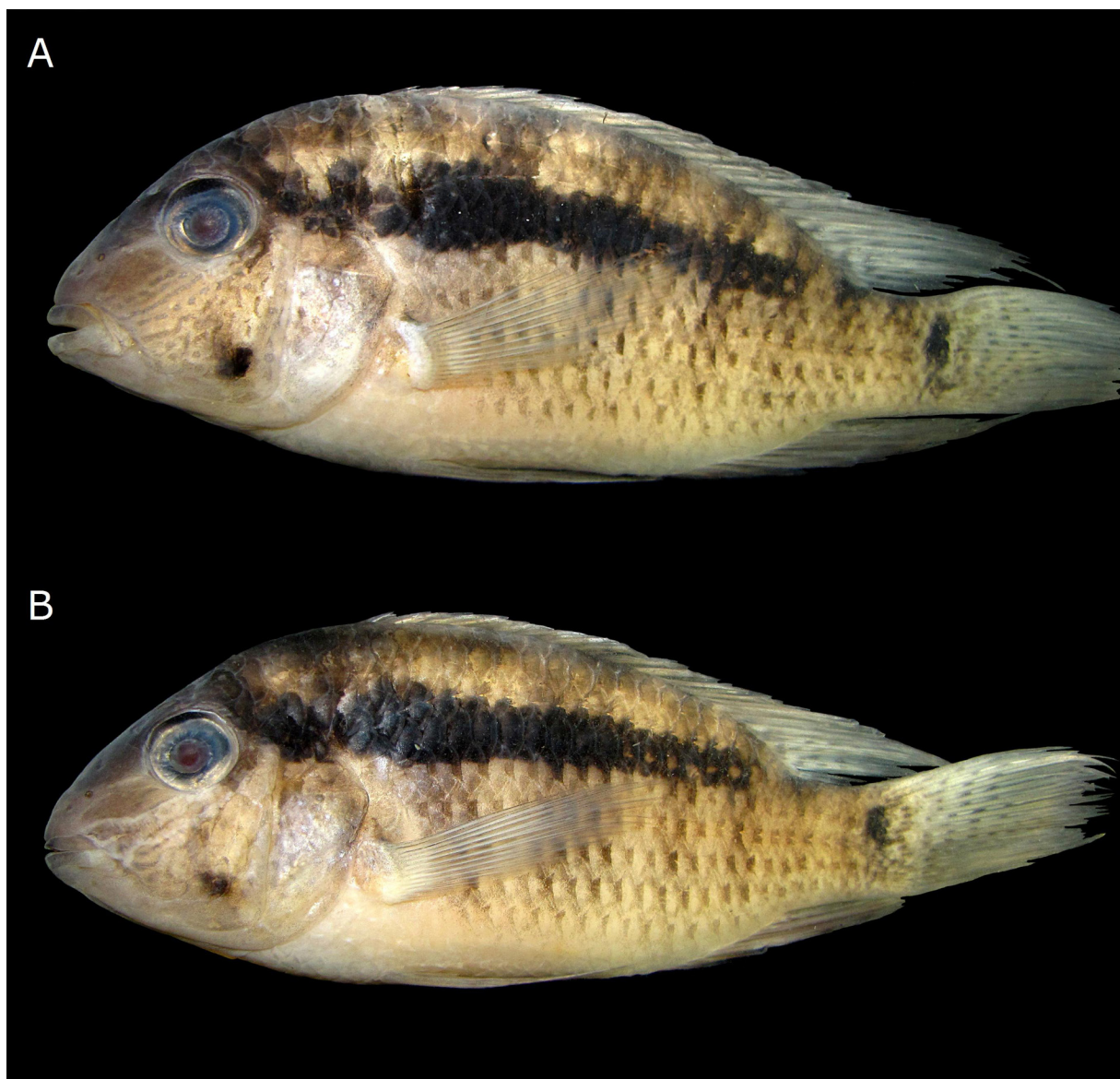


Fig. 8. *Bujurquina omagua* sp. nov., color photos of preserved specimens. **A.** Holotype (MUSM 70225, ID tag 1189), 97.4 mm. **B.** Paratype (MUSM 70226, P18-17_1190), 98.9 mm.

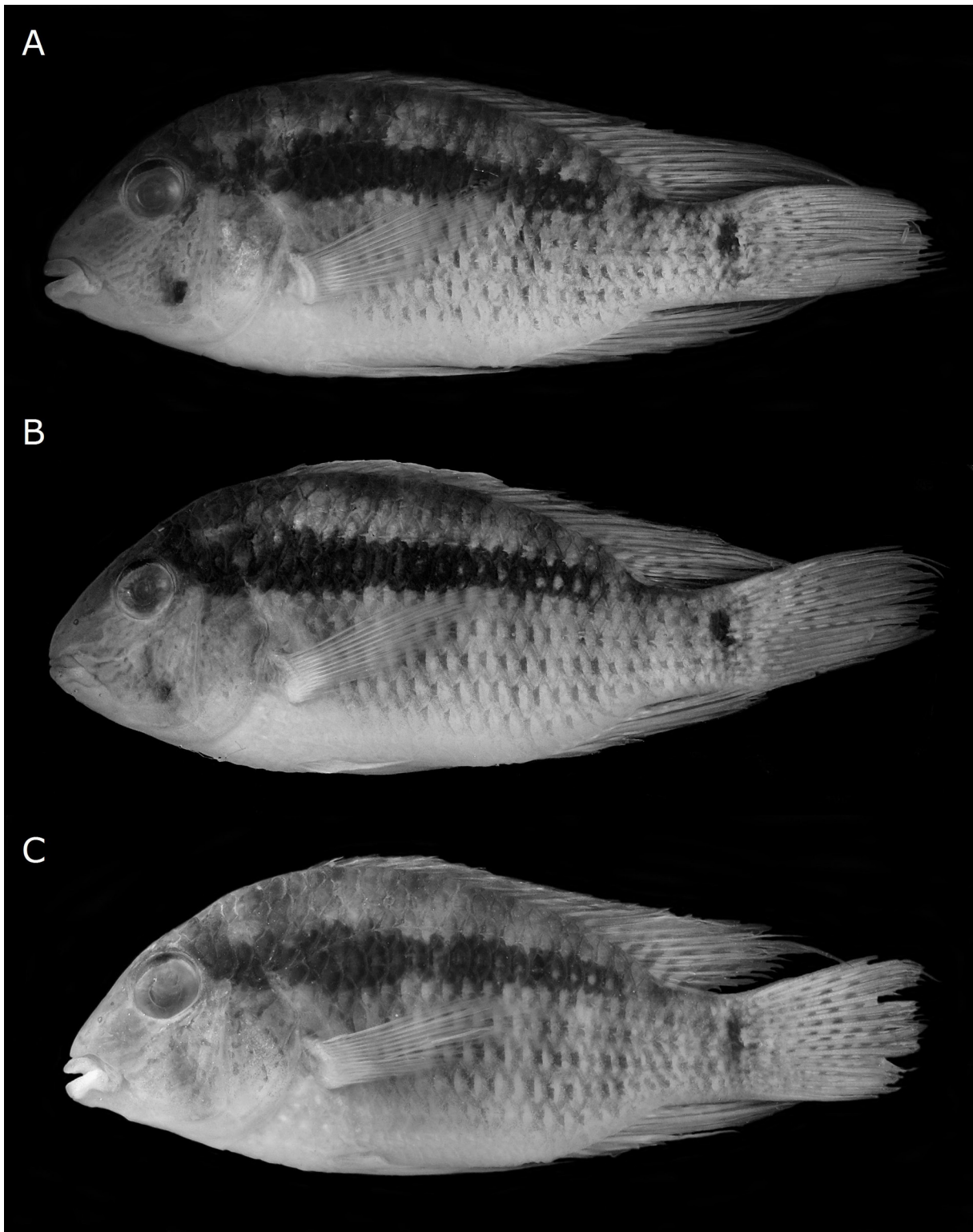


Fig. 9. *Bujurquina omagua* sp. nov., black and white photos of preserved specimens. **A.** Holotype (MUSM 70225, ID tag 1189), 97.4 mm. **B.** Paratype (MUSM 70226, P18-17_1190), 98.9 mm. **C.** Paratype (MUSM 70221, P18-15_1182), 78.7 mm.

Habitat

Bujurquina omagua sp. nov. was found only in small rainforest streams within the basins of the Sabalillo and Oran creeks. The localities (Fig. 11) were around 2 m wide streams, with shallow water (less than 1 m except in deeper pools) but deep mud and accumulated debris, blackish water, and only weak or moderate current. *Bujurquina omagua* has not been collected from the main streams of the Oran creek or from the lower sections of the Oran and Sabalillo creeks (Fig. 12), which have muddy water and where *B. sypilus* was found.

Distribution

Bujurquina omagua sp. nov. is only known from the Sabalillo and Oran creeks which empty into the Amazon River on either side of the village of Oran located on the first high ground just downstream from the mouth of the Napo into the Amazon, District Las Amazonas, Maynas Province, Department Loreto, Perú (Figs 1, 13).

Morphometric differentiation of *Bujurquina omagua* sp. nov.

Bujurquina omagua sp. nov. has a highly apomorphic head and body shape that sets it apart from the sympatric/parapatric species. When analyzed through PCA these species are arranged along the main tentic-lotic axis as corresponding to their lowland-upland habitats (Figs 14–15). The lotic/lentic ecomorphology dichotomy is in the PCA analyses best correlated with caudal peduncle length (long vs short), caudal peduncle depth (narrow vs deep), body depth (narrow vs deep), the size of the eye (orbital diameter; small vs large), pectoral fin length (short vs long), and last dorsal fin spine length (short vs long).

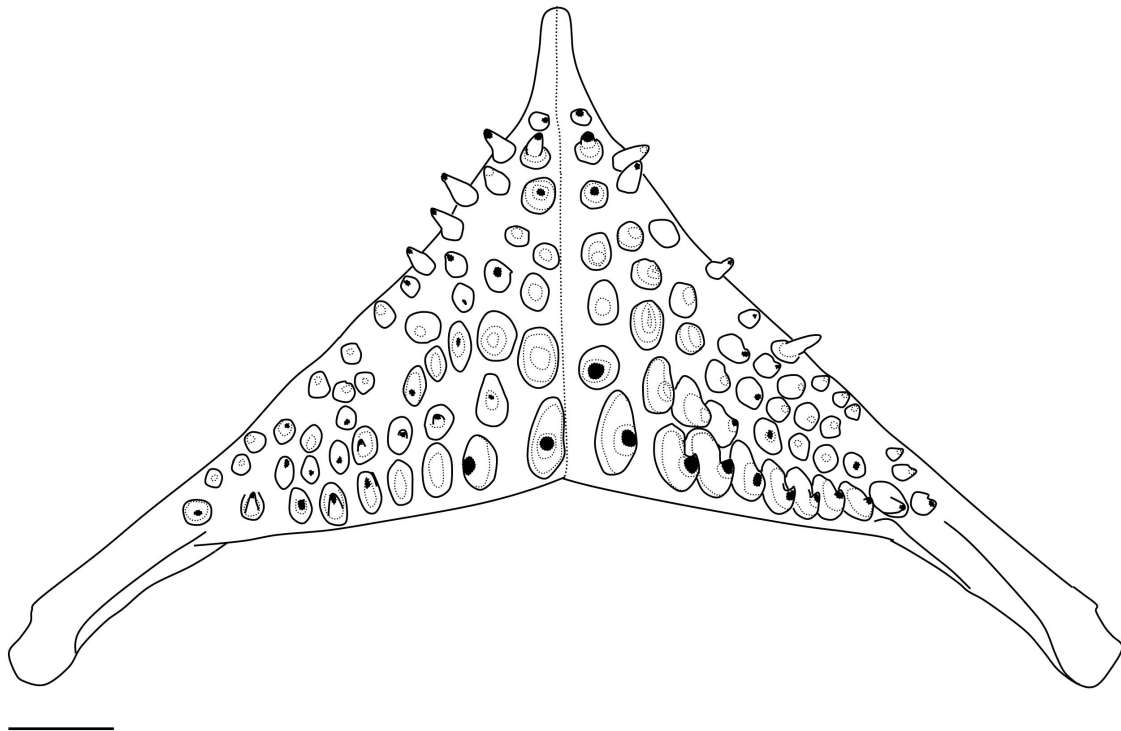


Fig. 10. *Bujurquina omagua* sp. nov., paratype (MUSM 70222, P18-16_1185, 79.9 mm), lower pharyngeal tooth plate in occlusal view. Scale bar = 1 mm.



Fig. 11. Type localities of *Bujurquina omagua* sp. nov. **A–B.** P18-15, Quebrada Sabalillo on trail from mouth, ($3^{\circ}27'45.6''$ S, $72^{\circ}29'22.5''$ W), 27th June 2018. **C.** P18-16, cabeceras of Quebrada Sabalillo, lower loc. ($3^{\circ}27'17.5''$ S, $72^{\circ}29'22.8''$ W), 28th June 2018. **D.** P18-17, holotype locality, cabeceras of Quebrada Sabalillo, upper loc. ($3^{\circ}27'08.4''$ S, $72^{\circ}29'11.8''$ W), 28th June 2018. **E.** P18-21, small unnamed quebrada just before entering Oran creek, ($3^{\circ}27'21.2''$ S, $72^{\circ}30'43.2''$ W), 3rd July 2018.

The remaining characters are not correlated with the main ecomorphological dichotomy (i.e., interocular distance, head width, head length, preorbital distance, snout length, and first ventral fin ray length) (Figs 14–15).

The lotic/lentic ecomorphology dichotomy is best visible in the analysis including all central western Amazonian species (Figs 1 and 14), while the diagnostic characters of *Bujurquina omagua* sp. nov. are best visible in the analysis excluding the westernmost and most highland species *B. zamorensis* (Fig. 15). *Bujurquina omagua* is in the PCAs distinguished from the sympatric/parapatric species predominantly by characters not correlated with the lotic-lentic, namely large head, wide head, long snout, and long preorbital distance. All these diagnostic characters are in line with the diagnosis of the species based on means and ranges of the morphometric characters (see above).

Bujurquina omagua sp. nov. has an outlying LPJ shape that can be described as the most delicate LPJ found among the valid species of *Bujurquina* (Fig. 16). The LPJ of *Bujurquina omagua* (studied in two specimens, see above) as expressed by proportional measurements is the shortest and widest of all species (L/W ratio) and the LPJ tooth-plate is the shortest in the genus (Ld/W ratio). Additionally to this the LPJ is very shallow vertically dorso-ventrally, but this character was scored as binary, in comparison to the length of teeth (see Results), and thus not included in the PCA analysis.

Paradoxically, the most delicate LPJ of *B. omagua* sp. nov. is associated with one of the largest heads among species of *Bujurquina* (together with *B. labiosa*) and with the longest snout among species of



Fig. 12. Lower portions of Sabalillo and Oran streams with muddy water with a blackish tinge (June 2018). *Bujurquina omagua* sp. nov. was not encountered in these habitats, which are typical for *B. sypilus* (Cope, 1872) in this area (see Fig. 13). **A.** Quebrada Sabalillo close to mouth into Amazon River. **B.** Oran creek at mouth of P18-21.

Bujurquina. A similar head and snout shape in *B. oenolaemus* is however associated with the most robust LPJ (Fig. 16) of this molluscivorous species.

A similar combination of a long snout and large head with a very delicate LPJ as in *B. omagua* sp. nov. is however also known from the cichlid genus *Australoheros* Říčan & Kullander, 2006 in the species *A. forquilha* Říčan & Kullander, 2008 and *A. ykeregua* Říčan, Piáleck, Almirón & Casciotta, 2011 (Říčan & Kullander 2008; Říčan *et al.* 2011).

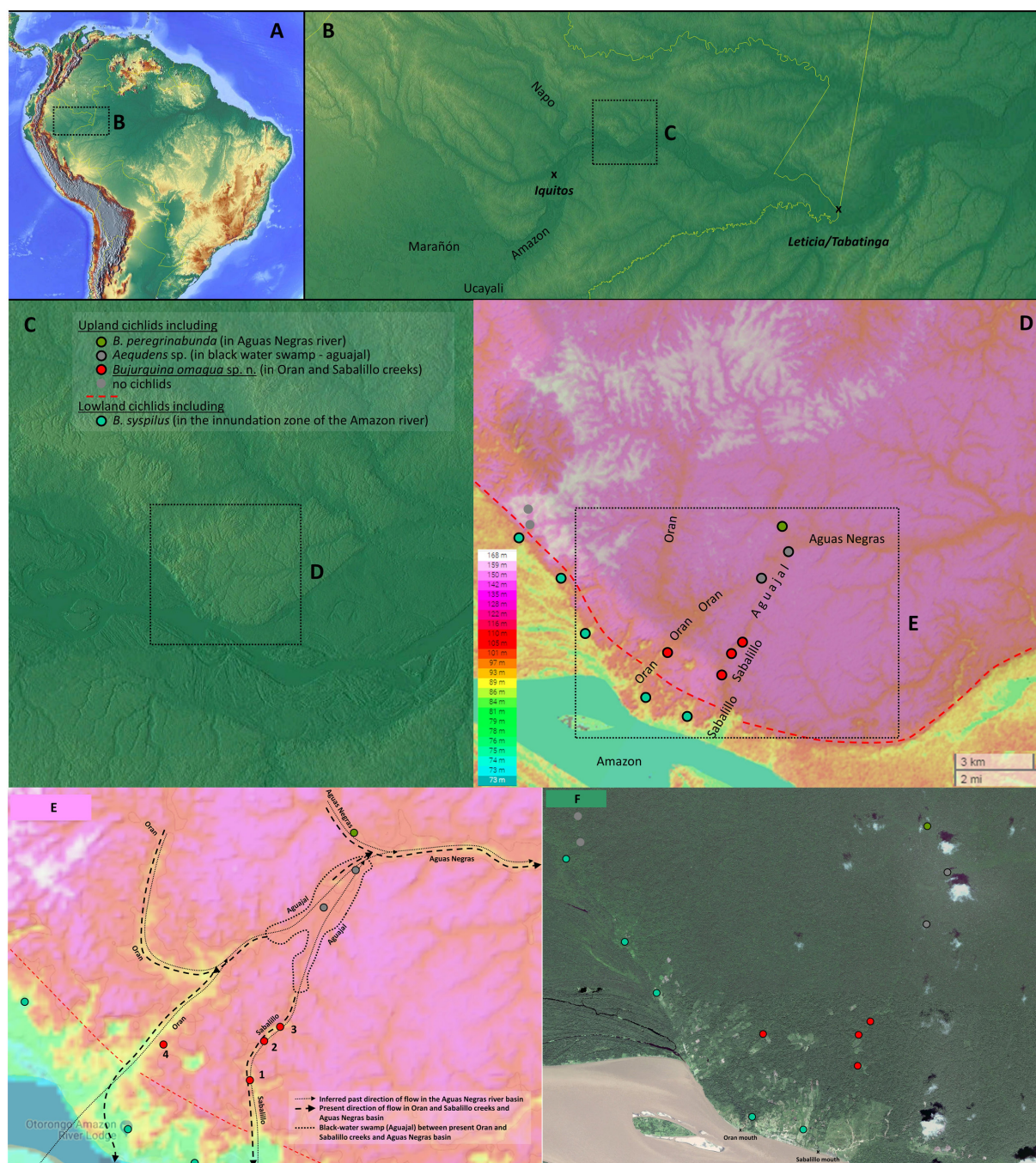


Fig. 13. Distribution of *Bujurquina omagua* sp. nov. and parapatric species in the so far whole known area close to Oran village, District Las Amazonas, Maynas Province, Department Loreto, Perú.

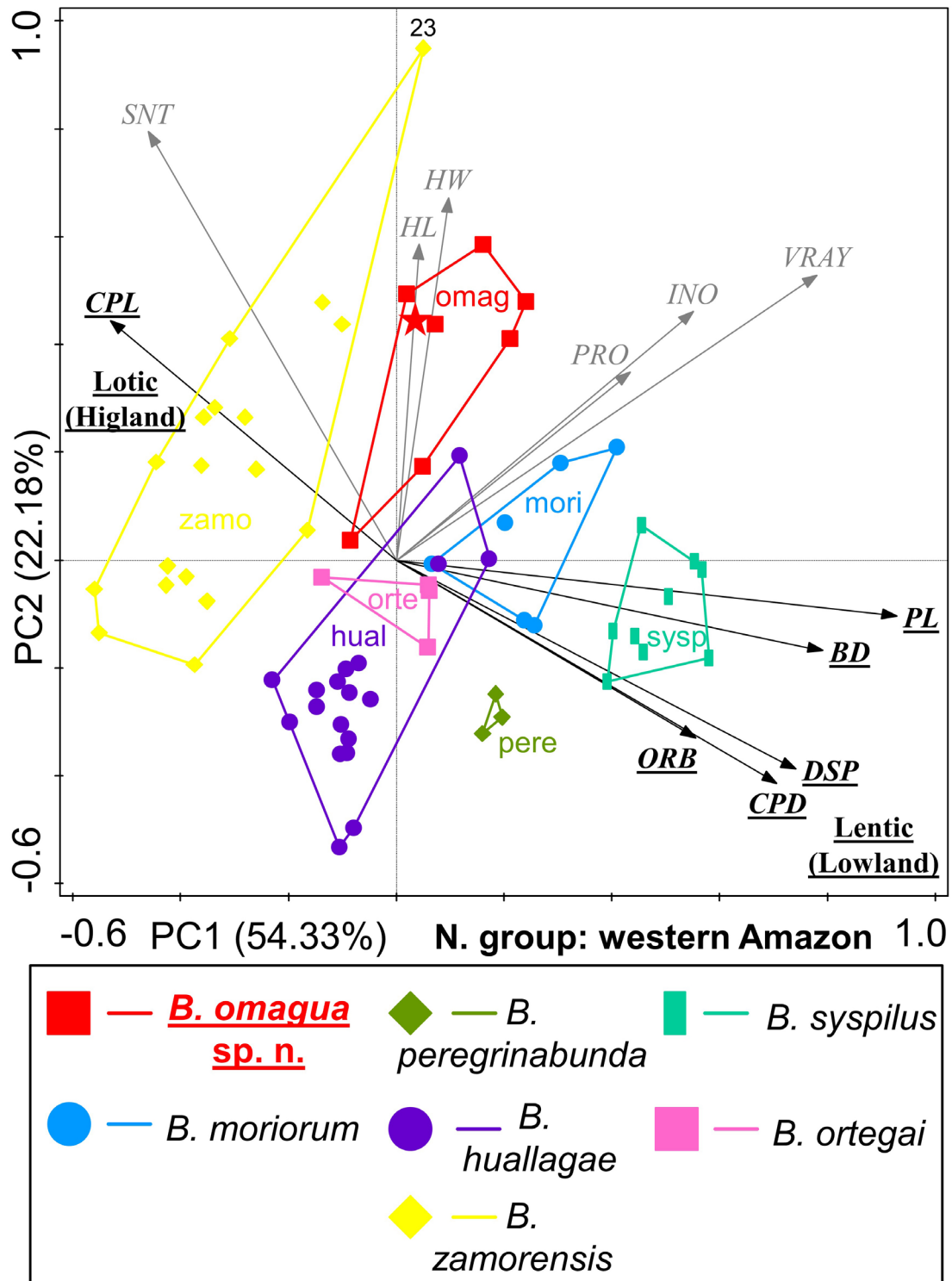


Fig. 14. Morphometric variation and discrimination of Northern group species in *Bujurquina* Kullander, 1986 from the western Amazon river basin based on morphometric proportional values of SL in PCA based on specimens ≥ 60 mm SL. Colors represent individual species. Note main separation along PC1 which also corresponds to two main ecomorphs (lotic and lentic). Note that *B. omagua* sp. nov. is separated from these geographically closest species by its large head. Note that *B. zamorensis* (Regan, 1905) is the most lotic and *B. sypsilus* (Cope, 1872) the most lentic species identified by the analysis.

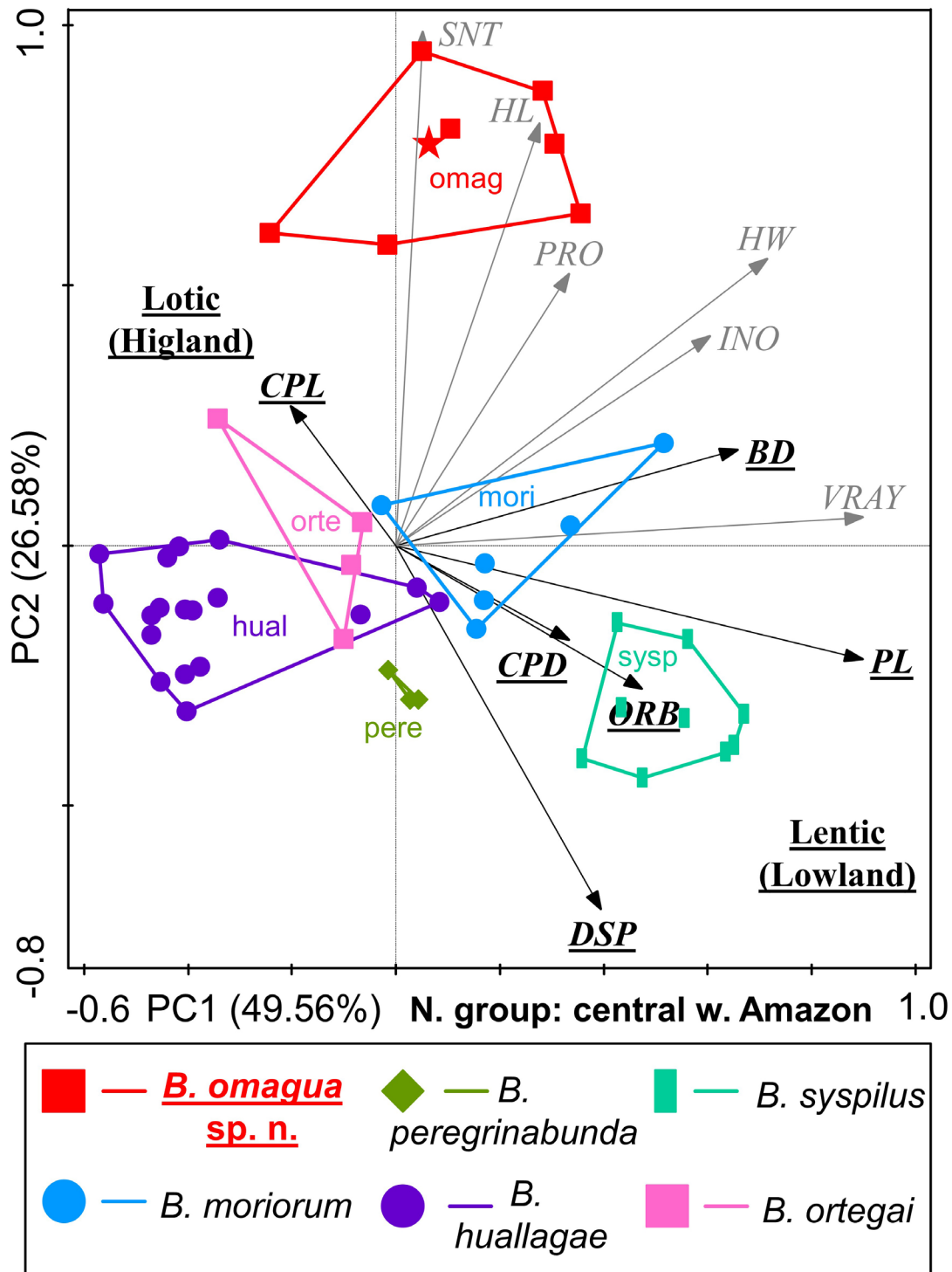


Fig. 15. Morphometric variation and discrimination of Northern group species in *Bujurquina* from the central western Amazon river basin (i.e., excluding *B. zamorensis* (Regan, 1905)) based on morphometric proportional values of SL in PCA based on specimens ≥ 60 mm SL. Colors represent individual species. Note main separation along PC1 which also corresponds to two main ecomorphs (lotic and lentic). Note that *B. omagua* sp. nov. is separated from these geographically closest species by its large head and long snout. Note improved separation of *B. huallagae* Kullander, 1986, *B. ortegai* Kullander, 1986 and *B. moriorum* Kullander, 1986 after exclusion of *B. zamorensis* (cf. Fig. 14).

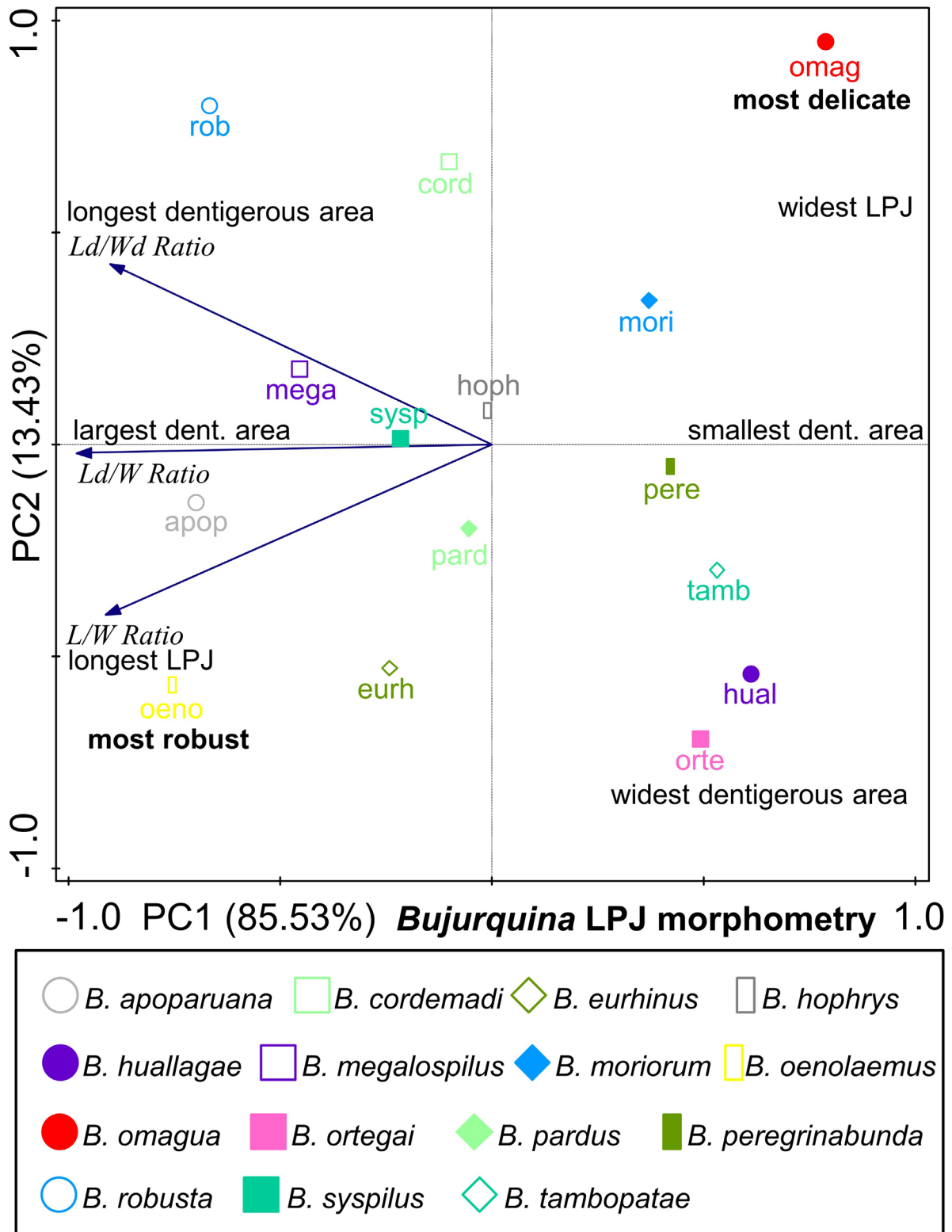


Fig. 16. PCA based on morphometric proportional values of LPJ of all described species in *Bujurquina* Kullander, 1986 based on specimens ≥ 60 mm SL. Colors represent individual species. Note that *B. omagua* sp. nov. has the most outlying LPJ shape.

Phylogeny of *Bujurquina* and phylogenetic position of *Bujurquina omagua* sp. nov.

Phylogenetic analyses of the 1055 characters *cytb* data matrix performed with MP in PAUP* (including all ingroup sequences) and BI analyses in MrBayes and BEAST (performed with the corresponding haplotypes data matrix) provided robust and very similar results. BI runs in independent analyses with the best-fitting model of evolution (GTR+I+G) converged well (ESS >200 for all parameters; burn-in 10%) and led to identical topologies under the same settings. The NJ and MP analyses were done with the complete dataset, the BI and BEAST analyses with the haplotype dataset. No phylogenetic differences were found between the MP, BI and BEAST analyses, and hence only the BEAST analysis is shown in Fig. 17.

The phylogenetic reconstructions divide *Bujurquina* into two main clades that can be diagnosed by patterned vs unpatterned dorsal fin, corresponding in geographical terms to Northern vs Southern group (Figs 1 and 17). The main biogeographic dichotomy within the genus between the Southern and Northern groups is within the present upper Ucayali basin in Peru (Fig. 1).

The two main clades of *Bujurquina* are dated as having diverged at 16.6 Ma. Within the Southern group the two southern-most species from Argentina, Paraguay, Brazil and Bolivia are sister species (*B. vittata* and *B. oenolaemus*), and they are a sister group to the clade composed of the Peruvian *B. eurhinus* and *B. tambopatae* as sister species, followed by the Bolivian *B. sp.* Bolivia and then the Peruvian *B. robusta*. The phylogenetically basal-most species of the Southern group is the Peruvian *B. labiosa*. The Peruvian species are thus in basal positions within the Southern group, and they also have the longest internodes

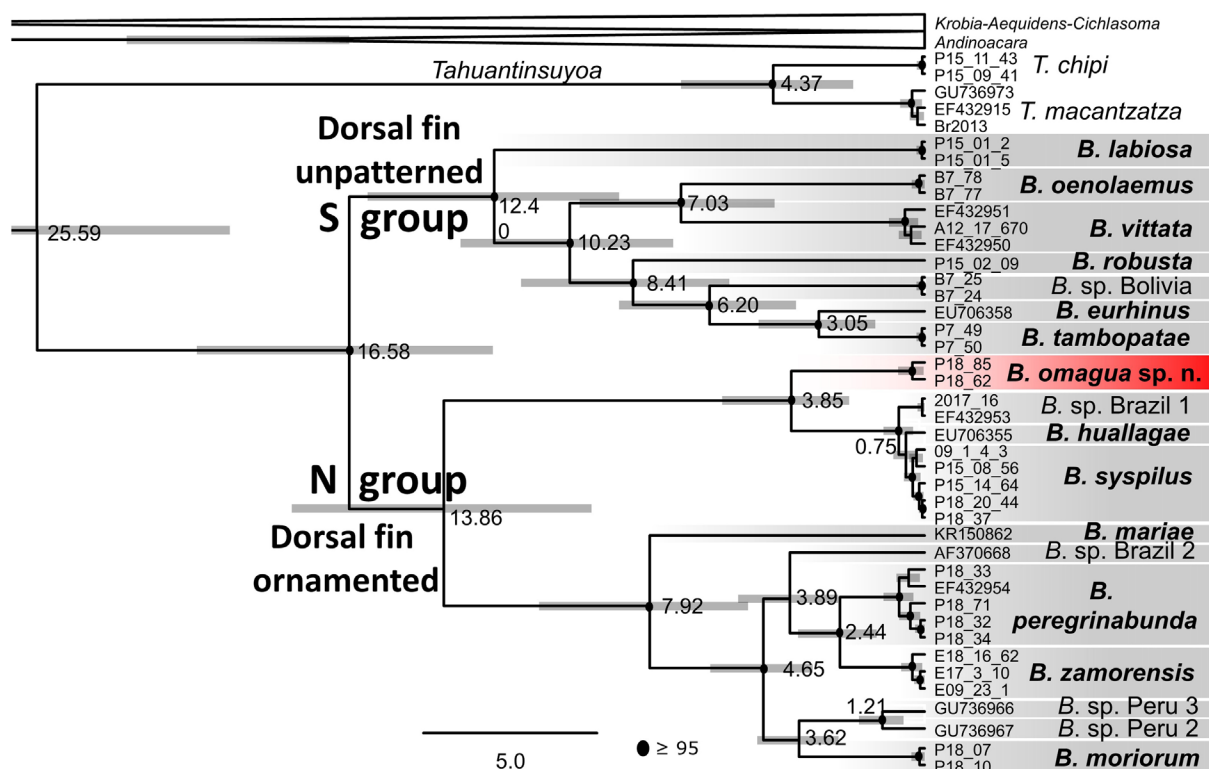


Fig. 17. Phylogenetic relationships and species delimitation within *Bujurquina* Kullander, 1986 based on the *cytb* marker from BEAST analysis. Numbers at nodes show age in Ma, grey bars at nodes show confidence intervals of age estimates (95% HPD). Bayesian posterior probabilities above 0.95 are shown as black points on nodes. Scale bar shows 5 My. Note the two main groups of *Bujurquina*.

and the earliest dates of divergence based on molecular clock dating, with the time frame of divergence among the Peruvian species dated between 12.4 Ma and 3.0 Ma (Fig. 17).

The Northern group of *Bujurquina* is made up of two highly divergent clades (Fig. 17) unlike the situation in the Southern group. The first clade within the Northern group shows a younger basal divergence at 3.9 Ma and includes, as a basal species, the here described *B. omagua* sp. nov., and then, among the Peruvian species, *B. huallagae* and *B. sypilus*. Samples of the morphologically and biogeographically Southern group species *B. megalospilus* are found within *B. sypilus* together with some samples of the Southern group species *B. labiosa* and *B. robusta* (Supp. file 2: Fig. S3). These three species clearly are Southern group species whose mtDNA in these particular samples was swept by mtDNA from *B. sypilus* following a single postulated hybridization event from *B. sypilus* into the three introgressed species, dated in our phylogeny at 0.2 Ma (cf. Fig. 17 and Supp. file 2: Fig. S3). Non-introgressed samples of *B. labiosa* and *B. robusta* are found as separate Southern group species in all phylogenetic analyses (see Fig. 17). Non-introgressed samples of *B. megalospilus* have not been found in this study. The close phylogenetic position in mtDNA of the morphologically dissimilar yet clearly Northern group species *B. sypilus* and *B. huallagae* may potentially also be a case of *B. sypilus* introgression into the sampled specimen of *B. huallagae*. This specimen was sampled in the lowermost portion of its distribution closest to the natural distribution of *B. sypilus* and not from the type locality of *B. huallagae* much higher up the namesake river.

In our present taxon sampling the first clade within the Northern group thus has a 10 my time gap from the basal node at 13.9 Ma to the presently sampled divergence at 3.9 Ma and this may suggest the existence of yet undiscovered older diverged species in this clade, or alternatively, it suggests extinction within the clade.

The second clade within the Northern group shows a younger basal divergence at 7.9 Ma, hence also with a time gap and with similar potential implications, which is strengthened by the isolated position of the basal-most species of this clade, *B. mariae* (Fig. 17). *Bujurquina mariae* (from Colombia) is the only species so far sampled from the Orinoco basin to the north of the Amazon basin. The two remaining Peruvian species (*B. peregrinabunda* and *B. moriorum*) diverged at 4.6 Ma, but they are not found as closely related in the mtDNA phylogeny despite being more similar and lowland parapatric species. Instead, the lowland *B. peregrinabunda* is found closely related to the allopatric Andean endemic *B. zamorensis* from Ecuador plus one putative lowland Ecuadorian species, most likely also found in Peru (*B. sp.* Ecuador 13). *Bujurquina moriorum* is found in a clade with two other putative Peruvian species from the Marañón basin.

Phylogeny and coloration patterns: the two main groups and phylogenetic lineages of Bujurquina

Our phylogenetic results have shown that *Bujurquina* is divided into two main clades. One clade, based on distribution patterns referred to us as the Northern group, is characterized by ornamented dorsal fins and a midlateral stripe running generally to the dorsal margin of the caudal peduncle (Figs 1, 4–5 and 17). In contrast to this the Southern group is characterized by unpatterned (hyaline, i.e., without any markings) dorsal fins and a midlateral stripe that always runs towards the posterior insertion of the dorsal fin (Figs 1–3 and 17). Lower lip coloration is another character that almost fully separates the two groups, since in majority of the Northern group species the lower lip is distinctly azure blue while in the Southern group species it is always the same color as the upper lip (i.e., never blue).

Key to the species of Bujurquina

For the key we have chosen to use only readily visible external characters. All characters except where specifically noted are for large adult specimens (usually above 60 mm SL), especially the color and

coloration pattern characters, where most are best visible in live specimens. In bold are the main distinguishing character states for each step.

1. Spinous portion of the dorsal fin ornamented (i.e., with blotches, lines etc.); midlateral stripe on body oriented towards posterior insertion of dorsal fin except in one species (*B. sypilus*), i.e., oriented nearly horizontally; flanks with dark, squarish or wedge-shaped spots, in overlapping region between scale base and overlying scale margin except in two species (*B. mariae* and *B. ortegai*) 2
 - Spinous portion of the dorsal fin **unpatterned** (i.e., hyaline without any markings); midlateral stripe on body oriented **towards soft portion** of dorsal fin, i.e., oriented more dorsally, flanks without spots 9
2. Spinous portion of the dorsal fin with **diagonal lines** (i.e., dark lines on a hyaline background) ... 3
 - Spinous portion of the dorsal fin with **circular markings** (i.e., hyaline blotches on a dark background) 6
3. Diagonal lines on spinous portion of the dorsal fin **thick**, sometimes barely recognisable as diagonal line but approaching blotches in shape, arranged as one longitudinal series with one line per membrane, dorsal-fin lappets orange; midlateral stripe on body oriented **towards soft portion** of dorsal fin; suborbital stripe vertical, in adults barely visible *B. sypilus* (Cope, 1872)
 - Diagonal lines on spinous portion of the dorsal fin **thin** 4
4. **Three** diagonal lines vertically on each membrane of spinous portion of the dorsal fin, each line spanning three consecutive membranes, lines oriented distinctly diagonal, about 45%, dorsal-fin lappets orange; suborbital stripe vertical, in adults distinct..... *B. mariae* (Eigenmann, 1923)
 - **One to two** diagonal lines per membrane on spinous portion of the dorsal fin 5
5. Lines per membrane oriented **only slightly diagonal**, two lines only in largest adult specimens, one line in dorsal portion of membrane in all other sizes, dorsal-fin lappets dark, with orange tip; suborbital stripe bent from vertical to posteriad in juveniles, reduced to a preopercular spot in adults; large head, length equal or above 36.3% SL; longest snout of all species without overlap (mean 15.5%, 14.4–16.4% of SL) *B. omagua* sp. nov.
 - Lines per membrane oriented **distinctly diagonal**, about 45%, dorsal-fin lappets nearly hyaline, only very slightly tinged orange; suborbital stripe slightly bent from vertical to posteriad, in adults well developed *B. ortegai* Kullander, 1986
6. Suborbital stripe **vertical** 7
 - Suborbital stripe **bent** from vertical to posteriad 8
 - Suborbital stripe **inclined** posteriad, in adults reduced to its ventral portion in the form of a short stripe or a preopercular spot; dorsal-fin lappets dark to black, not orange *B. moriorum* Kullander, 1986
7. Suborbital stripe **vertical, shifted posteriorly** to a position behind the eye, in adults always as a stripe, sometimes reduced only to its ventral portion; dorsal-fin lappets orange-brown, same color as rest of markings on dorsal fin, not orange *B. peregrinabunda* Kullander, 1986
 - Suborbital stripe **vertical**, in adults **whole**; dorsal-fin lappets orange-brown, same color as rest of markings on dorsal fin, not orange *B. huallagae* Kullander, 1986
8. Suborbital stripe **bent** from vertical to posteriad, in adults **reduced to an ocellated preopercular spot**; dorsal-fin lappets orange-brown, same color as rest of markings on dorsal fin, not orange *B. zamorensis* (Regan, 1905)
 - Suborbital stripe **bent** from vertical to posteriad, in adults **whole**; dorsal-fin lappets **white** with dark base *B. pardus* Arbour, Barriga Salazar & López-Fernández, 2014

9. Head **large**, length equal or above 37% SL 10
 – Head **small**, mean length below 35.5% SL 11
10. Mean length of head above 38.6% of SL, average 39.1%, lower pharyngeal teeth molariform, suborbital stripe in adults complete, dorsal-fin lappets white with dark base
 *B. oenolaemus* Kullander, 1987
 – Mean length of head above 37%, lips hypertrophied, suborbital stripe in adults incomplete, limited to below eye or to middle of cheek (does not reach angle of preopercle), dorsal-fin lappets white with dark base *B. labiosa* Kullander, 1986
11. Suborbital stripe in adults **complete** 12
 – Suborbital stripe in adults **incomplete** 13
 – Suborbital stripe in adults **reduced** to preopercular spot 14
 – Suborbital stripe in adults **absent**, dorsal-fin lappets **white** with dark base
 *B. eurhinus* Kullander, 1986
12. Suborbital stripe in adults **complete, distinct**, dorsal-fin lappets dark red to brown
 *B. vittata* (Heckel, 1840)
 – Suborbital stripe in adults **complete, indistinct**, dorsal-fin lappets distinctly **orange**
 *B. robusta* Kullander, 1986
 – Suborbital stripe **complete, indistinct**, dorsal-fin lappets **white** *B. cordemadi* Kullander, 1986
13. Suborbital stripe in adults **incomplete, limited to below eye**, weakly developed, dorsal-fin lappets **red** in anterior portion, **black** in posterior portion *B. megalospilus* Kullander, 1986
 – Suborbital stripe in adults **incomplete, limited to below eye**, weakly developed, dorsal-fin lappets **white** *B. tambopatae* Kullander, 1986
14. Suborbital stripe in adults **reduced** to preopercular spot, **well developed**, in most specimens clearly visible, dorsal-fin lappets with **dark** tips *B. hophrys* Kullander, 1986
 – Suborbital stripe in adults **reduced** to preopercular spot, **very weakly developed**, in most specimens almost invisible, dorsal-fin lappets with **dark orange** tips *B. apoparuana* Kullander, 1986

Discussion

Terra firme islands and floodplains and *Bujurquina* diversity in lowland Amazonia

Bujurquina omagua sp. nov. is the first new species of *Bujurquina* described from a terra firme island in the lowland Amazon. This however is not the only putative new species of *Bujurquina* known from a terra firme island. Several other are identified from the lowland area of Ecuadorian and northern Peruvian Amazonia. These are *B. peregrinabunda* and *B. moriorum* from the same general area as *B. omagua*, all three being separated by the floodplain species *B. sypsilus*. Among the undescribed species from the same area (Napo–Amazon) a lowland terra firme species is, e.g., *B.* sp. Ecuador 10 (= *B.* sp. Lower Curaray) while a sympatric floodplain species is *B.* sp. Ecuador 13 (= *B.* sp. Lower Pastaza-Morona) (Řičan *et al.* 2022).

The interplay between floodplain and terra firme species in *Bujurquina* in the lowland Amazon based on the recently obtained data presented here and in parallel studies (Řičan *et al.* 2022) appears to be not an exception but rather a rule and hence has great predictive power regarding areas for exploration that likely hide undescribed species. All areas of lowland western Amazonia so far explored for *Bujurquina* diversity host a more widespread lowland species found in the inundable area of the main rivers and tributaries, and then localized endemics found in streams of the terra firme islands that are separated (and hence effectively isolated in the case of *Bujurquina*) by the inundable areas of the main rivers.

The lowland Amazonian cichlid species including those of *Bujurquina* have been hypothesized to have larger distribution areas than the narrowly endemic foothill species (Kullander 1986). But the available data so far do not enable us to make this generalization because the lowlands of the western Amazon are still very sparsely explored for *Bujurquina* species diversity. Our newly collected high diversity of species in the Ecuadorian foothills (Říčan *et al.* 2022) supports narrow endemism in the foothills of the western Amazon also outside Peru for which it was initially formulated (Kullander 1986). In the western Amazonian lowlands the problems are twofold, large areas completely unexplored, and distribution limits of known species unknown. Hence comparisons to the foothill endemism are not yet possible. We actually do not know the distribution limits of a single lowland species of *Bujurquina* in the western Amazon, not from any of the megadiverse countries for *Bujurquina* (Peru, Ecuador). What appears to be the case is that we know that some lowland species, e.g., the floodplain species *B. syspilus*, do have a much larger distribution area than any of the foothill species, and this probably was at the core of the original formulation of the hypothesis. But the diversity of the terra firme species appears to be higher than the diversity of the floodplain species of *Bujurquina* and we simply do not know the sizes of any of the individual terra firme species distribution areas.

A reverse flowing river on a terra firme island

The modern Amazon River and its drainage basin were formed via some of the largest purported river capture events in Earth history that occurred during the late Miocene and Pliocene as signified by the appearance of the first Andean sediments in the Amazon Fan at about 10.1–9.4 Ma, with a large increase in sedimentation at about 4.5 Ma (Albert *et al.* 2018a).

River capture is a geomorphological process (*sensu* Gilchrist & Summerfield 1991; Bishop 2007) operating continually on most continental surfaces, whereby a portion of one river basin is diverted into a different drainage (Albert *et al.* 2018a). The effects of river capture on speciation and extinction are complex and intertwined, promoting both speciation and dispersal. As a result of these complex effects, river capture has been implicated in the formation of high freshwater diversity in many regions and taxa (Albert *et al.* 2018a, 2018b). Most of the ecosystems, clades and even species of Amazonian and in fact of many of Earth's ancient tropical biotas (e.g., Wiens & Donoghue 2004) are older than the geographic conditions in which they live today (Hoorn & Wesselingh 2010a, 2010b; Hoorn *et al.* 2010; Albert *et al.* 2011, 2018a; Graham 2011).

The here newly discovered and described species *B. omagua* sp. nov. is from a terra firme area just adjacent to the mouth of the present day Napo River into the Amazon River. Based on the river capture hypothesis that aims to explain the formation of the modern day Amazon and its drainage basin including the Napo River (see above) the presently W–E flowing Amazon and Napo rivers originated from a S–N flowing paleodrainage and mega-wetland around 4.5 Ma. This dating is supported by our molecular clock date of divergence of *B. omagua* (3.9 Ma). At 4.5 Ma the modern day Amazon (and Napo) rivers have cut through a high ground called the Iquitos arch forming the terra firme island on which *B. omagua* is found.

The Iquitos arch is one of several main structural arches (or swells) in the Amazon (Horbe *et al.* 2013) that prior to the origin of the modern Amazon formed topographic barriers or bounding structures to drainage basins (i.e., defined borders of drainage basins in lowland Amazonia). Structural arches are surface or sub-surface high or positive features caused by relative uplift over an elongated region that are formed by several different processes, including uplift from tectonic subduction, oroclinal bending, strike-slip faults, or forearc bulges, the Iquitos arch being an example of the last form (Albert *et al.* 2018a).

Our hypothesis for the reverse flowing river where *B. omagua* sp. nov. is found is that as the Amazon River at the time of its origin 4.5 Ma cut through the Iquitos arch it cut through the headwater portion of

a previously existing river system that had its southern headwaters on the Iquitos arch (Figs 1, 13). These now eroded headwaters on the Iquitos arch were the original southern headwaters of the present Aguas Negras River and the only parts of these southern tributaries that presently remain are the lower portions of the Oran and Saballilo creeks (Fig. 13D–E). These have reversed their flow direction (Fig. 13E) following the erosion of their original southern headwaters by the Amazon River augmented by the deepening and widening of the massive modern Amazon River valley. Following the reversal in flow direction of the Oran and Saballilo creeks a black water swamp (aguajal) developed in and around the former stream channels (Fig. 13E) that connected the original Oran and Saballilo tributaries to the Aguas Negras River.

Acknowledgements

We thank Hernán Ortega (Universidad Nacional Mayor de San Marcos, Lima, Perú) for enabling our collections in Peru and for long-term support of our projects in Peru. We also thank the people and guides from the village of Oran and the owners of the Otorongo Amazon river lodge, Ivonne Braga and Anthony Giardenelli, for logistic support. This study was partially supported by a DCG grant (Deutsche Cichliden-Gesellschaft) to OŘ.

References

- Albert J.S. & Reis R.E. (eds) 2011. *Historical Biogeography of Neotropical Freshwater Fishes*. University of California Press, Berkeley CA. <https://doi.org/10.1525/9780520948501>
- Albert J.S., Petry P. & Reis R.E. 2011. Major biogeographic and phylogenetic patterns. In: Albert J.S. & Reis R.E. (eds) *Historical Biogeography of Neotropical Freshwater Fishes*: 21–59. University of California Press, Berkeley. <https://doi.org/10.1525/9780520948501>
- Albert J.S., Val P. & Hoorn C. 2018a. The changing course of the Amazon River in the Neogene: center stage for Neotropical diversification. *Neotropical Ichthyology* 16 (3): e180033. <https://doi.org/10.1590/1982-0224-20180033>
- Albert J.S., Craig J.M., Tagliacollo V.A. & Petry P. 2018b. Upland and lowland fishes: a test of the River Capture Hypothesis. In: Hoorn C., Perrigo A. & Antonelli A. (eds) *Mountains, Climate and Biodiversity*: 273–294. Wiley Press, Cambridge.
- Arbour J.H., Barriga Salazar R.E. & López-Fernández H. 2014. A new species of *Bujurquina* (Teleostei: Cichlidae) from the Río Danta, Ecuador, with a key to the species in the genus. *Copeia* 2014: 79–86. <https://doi.org/10.1643/CI-13-028>
- Bishop P. 2007. Long-term landscape evolution: linking tectonics and surface processes. *Earth Surface Processes and Landforms* 32: 329–365. <https://doi.org/10.1002/esp.1493>
- Burress E.D., Alda F., Duarte A., Loureiro M., Armbruster J.W. & Chakrabarty P. 2018a. Phylogenomics of pike cichlids (Cichlidae: *Crenicichla*): the rapid evolution and trophic diversification of an incipient species flock. *Journal of Evolutionary Biology* 31 (1): 14–30. <https://doi.org/10.1111/jeb.13196>
- Burress E.D., Piálek L., Casciotta J.R., Almirón A., Tan M., Armbruster J.W. & Řičan O. 2018b. Island- and lake-like parallel adaptive radiations replicated in rivers. *Proceedings of the Royal Society B, Biological Sciences* 285: 20171762. <https://doi.org/10.1098/rspb.2017.1762>
- Bussing W.A. 1976. Geographical distribution of the San Juan ichthyofauna of Central America with remarks on its origin and ecology. In: Thorson T.B. (ed.) *Investigations of the Ichthyofauna of Nicaraguan Lakes*: 157–175. University of Nebraska, Lincoln, NE.

- Bussing W.A. 1985. Patterns of distribution of the Central American ichthyofauna. *In*: Stehli F.G. & Webb S.D. (eds) *The Great American Biotic Interchange*: 453–472. Plenum Publishing Corporation, New York. https://doi.org/10.1007/978-1-4684-9181-4_17
- Crampton W.G.R. 2011. An ecological perspective on diversity and distributions. *In*: Albert J.S. & Reis R.E. (eds) *Historical Biogeography of Neotropical Freshwater Fishes*: 165–189. University of California Press, Berkeley. <https://doi.org/10.1525/california/9780520268685.003.0010>
- Darlington Jr. P.J. 1957. *Zoogeography: The Geographical Distribution of Animals*. Wiley, New York.
- de Queiroz K. 2007. Species concepts and species delimitation. *Systematic Biology* 56: 879–886. <https://doi.org/10.1080/10635150701701083>
- Drummond A.J. & Rambaut A. 2007. BEAST: Bayesian evolutionary analysis by sampling trees. *BMC Evolutionary Biology* 7: 214. <https://doi.org/10.1186/1471-2148-7-214>
- Edgar R.C. 2004. MUSCLE: multiple sequence alignment with high accuracy and high throughput. *Nucleic Acids Research* 32: 1792–1797. <https://doi.org/10.1093/nar/gkh340>
- Ferraris C.J. 2007. Checklist of catfishes, recent and fossil (Osteichthyes: Siluriformes), and catalogue of siluriform primary types. *Zootaxa* 1418: 1–628. <https://doi.org/10.11646/zootaxa.1418.1.1>
- Gilchrist A.R. & Summerfield M.A. 1991. Denudation, isostasy and landscape evolution. *Earth Surface Processes and Landforms* 16: 555–562. <https://doi.org/10.1002/esp.3290160607>
- Graham A. 2011. The age and diversification of terrestrial New World ecosystems through Cretaceous and Cenozoic time. *American Journal of Botany* 98: 336–351. <https://doi.org/10.3732/ajb.1000353>
- Hellig C.J., Kerschbaumer M., Sefc K.M. & Koblmüller S. 2010. Allometric shape change of the lower pharyngeal jaw correlates with a dietary shift to piscivory in a cichlid fish. *Naturwissenschaften* 97 (7): 663–672. <https://doi.org/10.1007/s00114-010-0682-y>
- Hoorn C. & Wesselingh F.P. (eds) 2010a. *Amazonia: Landscape and Species Evolution: A Look into the Past*. Wiley-Blackwell, Chichester, UK. <https://doi.org/10.1002/9781444306408>
- Hoorn C. & Wesselingh F.P. 2010b. Introduction: Amazonia, landscape and species evolution. *In*: Hoorn C. & Wesselingh F.P. (eds) *Amazonia: Landscape and Species Evolution: A Look into the Past*. <https://doi.org/10.1002/9781444306408.ch1>
- Hoorn C.M., Wesselingh F.P., Ter Steege H., Bermudez M.A., Mora A., Sevink J., Sanmartín I., Sanchez-Meseguer A., Anderson C.L., Figueiredo J.P., Jaramillo C., Riff D., Negri F.R., Hooghiemstra H., Lundberg J., Stadler T., Särkinen T. & Antonelli A. 2010. Amazonia through time: Andean uplift climate change, landscape evolution and biodiversity. *Science* 330: 927–931. <https://doi.org/10.1126/science.1194585>
- Horbe A.M.C., Motta M.B., de Almeida C.M., Dantas E.L. & Vieira L.C. Provenance of Pliocene and recent sedimentary deposits in western Amazônia Brazil: consequences for the paleodrainage of the Solimões-Amazonas River. *Sedimentary Geology* 296: 9–20. <https://doi.org/10.1016/j.sedgeo.2013.07.007>
- Hubbell S.P., He F., Condit R., Borda-de-Agua L., Kellner J. & Ter Steege H. 2008. Colloquium paper: how many tree species are there in the Amazon and how many of them will go extinct? *Proceedings of the National Academy of Sciences of the USA* 105 (Supp. 1): 11498–11504. <https://doi.org/10.1073/pnas.0801915105>
- Huelsenbeck J.P. & Ronquist F. 2001. MrBayes: Bayesian inference of phylogenetics trees. *Bioinformatics* 17: 754–755. <https://doi.org/10.1093/bioinformatics/17.8.754>

- Ilves K.L., Torti D. & López-Fernández H. 2017. Exon-based phylogenomics strengthens the phylogeny of Neotropical cichlids and identifies remaining conflicting clades (Cichliformes: Cichlidae: Cichlinae). *Molecular Phylogenetics and Evolution* 118: 232–243. <https://doi.org/10.1016/j.ympev.2017.10.008>
- Kearse M., Moir R., Wilson A., Stones-Havas S., Cheung M., Sturrock S., Buxton S., Cooper A., Markowitz S., Duran C., Thierer T., Ashton B., Mentjies P. & Drummond A. 2012. Geneious basic: an integrated and extendable desktop software platform for the organization and analysis of sequence data. *Bioinformatics* 28: 1647–1649. <https://doi.org/10.1093/bioinformatics/bts199>
- Kullander S. 1986. *Cichlid Fishes of the Amazon River Drainage of Peru*. Swedish Museum of Natural History, Sweden.
- Kullander S.O. 1987. Cichlid fishes from the La Plata Basin. Part VI. Description of a new *Bujurquina* species from Bolivia. *Cybio* 1987: 195–205.
- Kullander S.O. 1996. *Heroina isonycterina*, a new genus and species of cichlid fish from Western Amazonia, with comments on cichlasomine systematics. *Ichthyological Exploration of Freshwaters* 7: 149–172.
- Kullander S.O., López-Fernández H. & van der Sleen P. 2018. Family Cichlidae – Cichlids. In: van der Sleen P. & Albert J.S. (eds) *Field Guide to the Fishes of the Amazon, Orinoco, and Guianas*: 359–385. Princeton University Press, New Jersey.
- Lucena C.A.S. & Kullander S.O. 1992. The *Crenicichla* (Teleostei: Cichlidae) species of the Uruguai River drainage in Brazil. *Ichthyological Exploration of Freshwaters* 3: 97–160.
- Musilová Z., Řičan O., Janko K. & Novák J. 2008. Molecular phylogeny and biogeography of the Neotropical cichlid fish tribe Cichlasomatini (Teleostei: Cichlidae: Cichlasomatinae). *Molecular Phylogenetics and Evolution* 46: 659–672. <https://doi.org/10.1016/j.ympev.2007.10.011>
- Musilová Z., Řičan O. & Novák J. 2009. Phylogeny of the Neotropical cichlid fish tribe Cichlasomatini (Teleostei: Cichlidae) based on morphological and molecular data, with the description of a new genus. *Journal of Zoological Systematics and Evolutionary Research* 47: 234–247. <https://doi.org/10.1111/j.1439-0469.2009.00528.x>
- Musilová Z., Řičan O., Řičanová Š., Janšta P., Gahura O. & Novák J. 2015. Phylogeny and historical biogeography of trans-Andean cichlid fishes (Teleostei: Cichlidae). *Vertebrate Zoology* 65: 333–350. <https://doi.org/10.3897/vz.65.e31524>
- Myers G.S. 1966. Derivation of the freshwater fish fauna of Central America. *Copeia* 4: 766–773. <https://doi.org/10.2307/1441405>
- Nylander J.A.A. 2004. *MrModeltest 2.2*. Evolutionary Biology Centre, Uppsala University, Sweden. Available from <http://www.abc.se/~nylander> [accessed 28 Apr. 2023].
- Oberdorff T., Dias M.S., Jezequel C., Albert J.S., Arantes C.C., Bigorne R., Carvajal-Valleros F.M., De Wever A., Frederico R.G., Hidalgo M., Hugueny B., Leprieur F., Maldonado M., Maldonado-Ocampo J., Martens K., Ortega H., Sarmiento J., Tedesco P.A., Torrente-Vilara G., Winemiller K.O. & Zuanon J. 2019. Unexpected fish diversity gradients in the Amazon basin. *Science Advances* 5 (9): eaav8681. <https://doi.org/10.1126/sciadv.aav8681>
- Piálek L., Burress E., Dragová K., Almirón A., Casciotta J. & Řičan O. 2019a. Phylogenomics of pike cichlids (Cichlidae: *Crenicichla*) of the *C. mandelburgeri* species complex: rapid ecological speciation in the Iguazú River and high endemism in the Middle Paraná basin. *Hydrobiologia* 832: 355–375. <https://doi.org/10.1007/s10750-018-3733-6>

- Piálek L., Casciotta J., Almirón A. & Říčan O. 2019b. A new pelagic predatory pike cichlid (Teleostei: Cichlidae: *Crenicichla*) from the *C. mandelburgeri* species complex with parallel and reticulate evolution. *Hydrobiologia* 832: 377–395. <https://doi.org/10.1007/s10750-018-3754-1>
- Rambaut A. & Drummond A.J. 2007. *Tracer 1.5.0*. Available from <http://beast.bio.ed.ac.uk/Tracer> [accessed 28 Apr. 2023].
- Reis R.E., Kullander S.O. & Ferraris Jr. C.J. 2003. *Check List of the Freshwater Fishes of South and Central America*. Edipucrs, Porto Alegre, Brazil.
- Říčan O. 2017. Sympatry and syntopy of cichlids (Teleostei: Cichlidae) in the Selva Central, upper Ucayali river basin, Peru. *Check List* 13 (3): 2146. <https://doi.org/10.15560/13.3.2146>
- Říčan O. & Kullander S.O. 2008. The *Australoheros* (Teleostei: Cichlidae) species of the Uruguay and Paraná River drainages. *Zootaxa* 1724: 1–51. <https://doi.org/10.11646/zootaxa.1724.1.1>
- Říčan O., Musilová Z., Muška M. & Novák J. 2005. Development of coloration patterns in Neotropical cichlids (Perciformes: Cichlidae: Cichlasomatinae). *Folia Zoologica* 54: 1–46.
- Říčan O., Zardoya R. & Doadrio I. 2008. Phylogenetic relationships of Middle American cichlids (Teleostei, Cichlidae, Heroini) based on combined evidence from nuclear genes, mtDNA, and morphology. *Molecular Phylogenetics and Evolution* 49: 941–958. <https://doi.org/10.1016/j.ympev.2008.07.022>
- Říčan O., Piálek L., Almirón A. & Casciotta J. 2011. Two new species of *Australoheros* (Teleostei: Cichlidae), with notes on diversity of the genus and biogeography of the Río de la Plata basin. *Zootaxa* 2982: 1–26. <https://doi.org/10.11646/zootaxa.2982.1.1>
- Říčan O., Piálek L., Zardoya R., Doadrio I. & Zrzavý J. 2013. Biogeography of the Mesoamerican Cichlidae (Teleostei: Heroini): colonization through the GAARlandia land bridge and early diversification. *Journal of Biogeography* 40: 579–593. <https://doi.org/10.1111/jbi.12023>
- Říčan O., Piálek L., Dragová K. & Novák J. 2016. Diversity and evolution of the Middle American cichlid fishes (Teleostei: Cichlidae) with revised classification. *Vertebrate Zoology* 66: 1–102. <https://doi.org/10.3897/vz.66.e31534>
- Říčan O., Říčanová Š., Dragová K., Piálek L., Almirón A. & Casciotta J. 2019. Species diversity in *Gymnogeophagus* (Teleostei: Cichlidae) and comparative biogeography of cichlids in the Middle Paraná basin, an emerging hotspot of fish endemism. *Hydrobiologia* 832: 331–354. <https://doi.org/10.1007/s10750-018-3691-z>
- Říčan O., Dragová K., Almirón A., Casciotta J., Gottwald J. & Piálek L. 2021. MtDNA species-level phylogeny and delimitation support significantly underestimated diversity and endemism in the largest Neotropical cichlid genus (Cichlidae: *Crenicichla*). *PeerJ* 9: e12283. <https://doi.org/10.7717/peerj.12283>
- Říčan O., Říčanová Š., Rodriguez Haro L.R. & Rodriguez Haro C.E. 2022. Unrecognized species diversity and endemism in the cichlid genus *Bujurquina* (Teleostei: Cichlidae) together with a molecular phylogeny document large-scale transformation of the western Amazonian river network and reveal complex paleogeography of the Ecuadorian Amazon. *Hydrobiologia*. <https://doi.org/10.1007/s10750-022-05019-z>
- Ronquist F. & Huelsenbeck J.P. 2003. MrBayes 3: Bayesian phylogenetic inference under mixed models. *Bioinformatics* 19:1572–1574. <https://doi.org/10.1093/bioinformatics/btg180>
- Sabaj M.H. 2020. Codes for Natural History Collections in Ichthyology and Herpetology. *Copeia* 108: 593–669. <https://doi.org/10.1643/ASIHCODONS2020>

- Šmilauer P. & Lepš J. 2014. *Multivariate Analysis of Ecological Data using Canoco 5*. Cambridge University Press, New York. <https://doi.org/10.1017/CBO9781139627061>
- Stawikowski R. & Werner U. 1998. *Die Buntbarsche Amerikas, Band 1*. Eugen Ulmer Verlag, Stuttgart.
- Stawikowski R. & Werner U. 2004. *Die Buntbarsche Amerikas. Band 3: Erdfresser, Hecht-und Kambuntbarsche*. Eugen Ulmer Verlag, Stuttgart.
- Swofford D.L. 2003. *PAUP*: Phylogenetic Analysis Using Parsimony (*and other methods), version 4.0b10*. Sinauer Associates, Sunderland, MA.
- Toivonen T., Mäki S. & Kalliola R. 2007. The riverscape of Western Amazonia – A quantitative approach to the fluvial biogeography of the region. *Journal of Biogeography* 34: 1374–1387. <https://doi.org/10.1111/j.1365-2699.2007.01741.x>
- Van der Sleen P. & Albert J.S. 2018. *Field Guide to the Fishes of the Amazon, Orinoco, and Guianas*. Princeton University Press, New Jersey. <https://doi.org/10.1515/9781400888801>
- Villesen P. 2007. FaBox: an online toolbox for FASTA sequences. *Molecular Ecology Notes* 7 (6): 965–968. <https://doi.org/10.1111/j.1471-8286.2007.01821.x>
- Wallace A.R. 1876. *The Geographical Distribution of Animals; with a Study of the Relations of Living and Extinct Faunas as Elucidating the Past Changes of the Earth's Surface*. Two volumes. Harper & Brothers, New York. <https://doi.org/10.5962/bhl.title.46581>
- Wesselingh F.P. & Hoorn C. 2011. Geological development of Amazon and Orinoco Basins. In: Albert J. S. & Reis R.E. (eds) *Historical Biogeography of Neotropical Freshwater Fishes*: 59–67. University of California Press, Berkeley, CA.
- Wiens J.J. & Donoghue M.J. 2004. Historical biogeography ecology and species richness. *Trends in Ecology and Evolution* 19: 639–644. <https://doi.org/10.1016/j.tree.2004.09.011>

Manuscript received: 20 July 2022

Manuscript accepted: 23 January 2023

Published on: 1 June 2023

Topic editor: Tony Robillard

Section editor: Felipe Polivanov Ottoni

Desk editor: Pepe Fernández

Printed versions of all papers are also deposited in the libraries of the institutes that are members of the *EJT* consortium: Muséum national d'histoire naturelle, Paris, France; Meise Botanic Garden, Belgium; Royal Museum for Central Africa, Tervuren, Belgium; Royal Belgian Institute of Natural Sciences, Brussels, Belgium; Natural History Museum of Denmark, Copenhagen, Denmark; Naturalis Biodiversity Center, Leiden, the Netherlands; Museo Nacional de Ciencias Naturales-CSIC, Madrid, Spain; Leibniz Institute for the Analysis of Biodiversity Change, Bonn – Hamburg, Germany; National Museum of the Czech Republic, Prague, Czech Republic.

Supplementary material

Supp. file 1. Table S1. Specimens included in the study. <https://doi.org/10.5852/ejt.2023.870.2127.8993>

Supp. file 2. Additional information. <https://doi.org/10.5852/ejt.2022.870.2127.8995>

Fig. S1. Photos of live specimens of described species of *Bujurquina* Kullander, 1986. The only species missing are *B. pardus* Arbour, Barriga Salazar & López-Fernández, 2014 and *B. cordemadi* Kullander, 1986. This is the first time photos of virtually all described species are presented, since for most species the live appearance is not known, and for those where it is, it is not from type localities or close to them as presented here.

Fig. S2. Outgroups of phylogenetic analysis showing calibration nodes (in yellow) and resulting dating estimates for these nodes (in green) in the final phylogenetic analysis from BEAST (Fig. 17). Tree is NJ topology, values at nodes are MP bootstrap.

Fig. S3. Introgressed samples of the morphologically and biogeographically Southern group species *B. megalospilus* Kullander, 1986, *B. labiosa* Kullander, 1986 and *B. robusta* Kullander, 1986 found in exploratory NJ analysis within the Northern group species *B. sypilus* (Cope, 1872). Non-introgressed samples of *B. labiosa* and *B. robusta* are found as separate Southern group species in all phylogenetic analyses (see Fig. 17). Non-introgressed samples of *B. megalospilus* have not been found in this study. Values at nodes are MP bootstrap. Only part of the NJ tree is shown for clarity.

Table S2. Table of proportional measurements in percent of standard length in described species of *Bujurquina* Kullander, 1986. The table includes specimens above 40 mm SL, PCA from these data (Figs 12–15) are based on specimens above 60 mm SL, except *B. cordemadi* Kullander, 1986, *B. labiosa* Kullander, 1986, *B. megalospilus* Kullander, 1986, *B. oenolaemus* Kullander, 1987, and *B. vittata* (Heckel, 1840) where some specimens between 50 and 60 mm SL were used because of lack of enough larger specimens. Data for *B. pardus* Arbour, Barriga Salazar & López-Fernández, 2014 is from Arbour *et al.* (2014) and for *B. cordemadi* from Kullander (1986). Colors aid in visualizing delimitation of the described species from *B. omagua* sp. nov. Values in orange are smaller than in *B. omagua* and show no overlap between *B. omagua* and the given species, values in green are larger than in *B. omagua* and also show no overlap. Values in orange and red are thus diagnostic between *B. omagua* and the described species. Values in grey are not strictly diagnostic, those in dark grey provide tendency towards separation while those in light grey provide no separation. Abbreviation: SD = standard deviation.